In presenting the dissertation as a partial fulfillment of the requirements for an advanced degree from the Georgia Institute of Technology, I agree that the Library of the Institute shall make it available for inspection and circulation in accordance with its regulations governing materials of this type. I agree that permission to copy from, or to publish from, this dissertation may be granted by the professor under whose direction it was written, or, in his absence, by the Dean of the Graduate Division when such copying or publication is solely for scholarly purposes and does not involve potential financial gain. It is understood that any copying from, or publication of, this dissertation which involves potential financial gain will not be allowed without written permission.

_____

_____

7/25/68

THERMOELASTIC EFFECTS OF THE ELEMENTS IN COMPRESSION

A THESIS

Presented to

The Faculty of the Graduate Division

by

Ramesh Chandra Lal

In Partial Fulfillment

of the Requirements for the Degree

Master of Science in Metallurgy

Georgia Institute of Technology

June, 1970

THERMOELASTIC EFFECTS OF THE ELEMENTS IN COMPRESSION

Approved:

Chairman

Date approved by Chairman: June 17-70

ACKNOWLEDGMENTS

It is the pleasant duty of the author to express his gratitude to those who have assisted him in completing this work.

The author records his indebtedness to Dr. Niels Engel, as the supervisor of this research project, who proved a perennial source of dedicated help, encouragement and new ideas.

Heartfelt thanks are also due to Dr. S. Spooner and Dr. Helen Grenga for their constructive suggestions and advice in presenting this study.

A good deal of appreciation goes to Mr. Charlie Blackwood of workshop for his personal interest and help in making many items required in this investigation.

Lastly, the author wishes to express his admiration and thanks to his wife (Mohini) and child (Rakesh) for their cooperation, inspiration and active help in performing the experiments at many odd hours.

TABLE OF CONTENTS

Page

ACKNOWLEDGMENTS ii

LIST OF TABLES v

LIST OF ILLUSTRATIONS vi

SUMMARY viii

Chapter

I. HISTORICAL INTRODUCTION 1

Survey over Bonding Mechanisms
Theories of Metallic Bonding and Engel Concepts

II. THEORETICAL BACKGROUND 17

III. EXPERIMENTAL WORK 25

General Principle
Instrumentation
Device for Temperature Measurement and Calibration
Device for Pressure Measurement and Calibration
Preparation of Specimen

IV. DISCUSSION OF RESULTS 41

Errors in Measurement
Evaluation of Experimental Results
Thermoelastic Effect

V. CONCLUSIONS AND RECOMMENDATIONS 67

APPENDICES 71

A. ENERGY ABSORBED BY ELECTRON GAS IN COMPRESSING Na 72

TABLE OF CONTENTS (Continued)

Page

APPENDICES (Continued)

B. CALCULATIONS OF TEMPERATURE CALIBRATION 75

C. CALCULATIONS OF PRESSURE CALIBRATION 77

D. A TYPICAL CALCULATION OF ADIABATIC HEAT OF COMPRESSION 79

E. A TYPICAL CALCULATION OF MECHANICAL WORK INPUT TO SPECIMEN 81

F. A TYPICAL CALCULATION OF $\Delta T/\Delta P$ FROM THERMOELASTIC EQUATION 84

BIBLIOGRAPHY 96

LIST OF TABLES

Table		Page
1.	Physical Constants Used	86
2.	Experimental Values.	89
3.	Observed and Calculated Values of $\frac{\Delta T}{\Delta P}$	93
4.	Promotion Energies of $d^{n-2}sp$ Valence State	94
5.	Promotion Energies of $d^{n-1}s$ Valence State	95

LIST OF ILLUSTRATIONS

Figure		Page
1.	Bonding Mechanism in Metals	5
2.	Melting Point of the Fourth Period Elements	13
3.	Melting Point of the Fifth Period Elements	14
4.	Melting Point of the Sixth Period Elements	15
5.	Atomic Distance of the Fourth Period Elements	19
6.	Atomic Distance of the Fifth Period Elements	19
7.	Atomic Distance of the Sixth Period Elements	20
8.	Schematic Setup of Pressure Vessel and Heat Output Measurement	26
9a.	Arrangements of Punch Press Machine, Pressure Vessel and Electrical Gadgetry	27
9b.	A Closeup of Pressure Vessel, Valve and Pressure Cell	28
10.	Specimen Holders and Specimen	29
11.	Details of Insulated Heat Output System	30
12.	Layout of Principal Instruments	32
13.	Circuit Diagram for Temperature Calibration	35
14.	Pressure Cell Circuit in Conjunction with a Device for Voltage Multiplication Factor	35
15.	Pressure Effect Measured as a Differential of Pressure Change	42
16.	Typical Curves of Temperature Calibration and of Temperature and Pressure Variations	45

LIST OF ILLUSTRATIONS (Continued)

Figure		Page
17.	Comparison of the Observed and Calculated Values of $\Delta T/\Delta P$ in the Second, Third, Sixth-a and Seventh Period Elements	47
18.	Comparison of the Observed and Calculated Values of $\Delta T/\Delta P$ in the Fourth Period Elements	48
19.	Comparison of the Observed and Calculated Values of $\Delta T/\Delta P$ in the Fifth Period Elements	49
20.	Comparison of the Observed and Calculated Values of $\Delta T/\Delta P$ in the Sixth Period Elements.	50
21.	Thermoelastic Behavior of Elements in Compression over Second, Third, Sixth-a and Seventh Periods	51
22.	Thermoelastic Behavior of Elements in Compression over Fourth Period.	52
23.	Thermoelastic Behavior of Elements in Compression over Fifth Period	53
24.	Thermoelastic Behavior of Elements in Compression over Sixth Period	54
25.	Thermoelastic Behavior of Cs in Compression at Different Working Temperatures.	55
26.	Distribution of the Ratio of Observed to Calculated Value of $\Delta T/\Delta P$ in Fourth, Fifth and Sixth Period Elements	58
27.	Relative Promotion Energy of $d^{n-1}s$ and $d^{n-2}sp$ Electronic Configurations for the Fourth Period Elements	63
28.	Relative Promotion Energy of $d^{n-1}s$ and $d^{n-2}sp$ Electronic Configurations for the Fifth Period Elements	64
29.	Relative Promotion Energy of $d^{n-1}s$ and $d^{n-2}sp$ Electronic Configurations for the Sixth Period Elements	65

SUMMARY

It has been known that the electronic configurations of elements change under pressure. It may also lead to change in structure or lattice. An investigation of adiabatic heat of compression of elements will be conducive to know the movement of electrons between shells in the elements with respect to pressure. As such, we are measuring the adiabatic heat of compression of different elements with a particular emphasis on pure metals. A pressure of about 3, 000 p. s.i. is being used for this purpose. This heat of compression will be calculated in the following manner:

Heat output - Mechanical Work input = Change of Internal Energy

Heat output is the temperature increase due to compression multiplied by the specific heat of the material.

It is hoped that our results would help reveal the actual bonding mechanism of metals. According to the Engel concepts, bonding electrons should exist both in the d and outer (s+p) shells in the transition metals. Pressure should cause electrons to move between energy levels. Due to the promotion energy such movements should be measurable as part of the change of internal energy.

CHAPTER I

HISTORICAL INTRODUCTION

The history and development of science has been the same as that of mankind. Endowed with power, man went on unfolding the secret but poignant story of Nature. Thus science made rapid strides in the hands of man and not as his brainchild. Several theories were propounded to explain the observed facts. With the severe impact of new and better convincing ideas, some old concepts were dislodged; but some survived possibly because of their solid base. To the utter shock and dismay of many rational thinkers and scientists, some theories are still deep-rooted and heavily protected by scientific bigots and demagogs despite their numerous proven shortcomings and fallacies. "Ring out the old--ring in the new" seems to be the desirable guideline for the true development of science.

In the following pages, attempts will be made to explain a specific group of well-established scientific facts in the light of "cause-effect" phenomenon.

Survey over Bonding Mechanisms

Different types of bonding forces hold the atoms together in solid state such as the Van der Waal's bond, the ionic bond and the covalent bond (metallic and non-metallic).

The unsymmetrical or unbalanced distribution of electrons around the nucleus creates oscillating electrical dipoles. The force produced between the

opposite ends of dipoles in neighboring atoms or molecules tends to attract them together. In other words, the interaction of these dipoles gives rise to the Van der Waal's bond. In comparison to chemical bonding like covalent and ionic bonds, the Van der Waal's forces of bonding are weak and short-ranged. These forces also occur between neutral atoms. In the event of chemical bonding amongst atoms in solid state, the Van der Waal's forces play a negligible role in the determination of atomic lattices as contrasted to molecular lattices.

A structure held together by ionic bonds takes place when there is a mutual electron transfer between atoms. Such bonds usually develop when atoms from extreme left in the periodic table are allowed to mix with atoms from extreme right. The atoms of the alkali or alkaline metals strip off their outer electrons which in turn are accepted by the halogene or chalcogene atoms in their empty quantum states in the outer partly filled shells. Within an ionic structure two kinds of forces dominate because of the existence of the charged particles or ions. One kind of force is an electrostatic attraction and repulsion between positively and negatively charged ions. This force is essentially scalar in nature, and is inversely proportional to the square of the distance between the two charged ions. On the other hand, when the ions are brought very close to each other resulting in the overlap of outer electronic shells, a repulsive force in the range of r^6 to r^{12} (r being the ionic radius) is generated.

Ionic or polar crystals form in such a fashion that the distance between oppositely charged ions is least and the distance between equally charged ions is greatest. For ionic crystals Born (1) and Madelung (2) proposed that when the

forces of electrostatic attraction and repulsion (caused by shell overlap) balance each other, an equilibrium distance between the oppositely charged ions is obtained. In case of ionic bonding, it would seem that (a) the electron transfer tends to make complete outer electronic shells; (b) there is electrostatic attraction between ions formed; (c) great repulsive forces keep the ions at a distance when the complete shells make mutual contact.

Goldschmidt (3) showed that the formation of ionic lattices depend on the atomic size factor or the ratio of ionic diameters. For example, NaCl and CsCl exhibit the same electronic pattern, but they differ in lattice type. In CsCl lattice, the ionic size ratio is unity and has a coordination number 8; whereas NaCl lattice has an ionic size ratio not equal to unity and has a coordination number 6.

G. N. Lewis (4, 5) proposed the electron pair covalent bond theory in 1916. This was further developed by Linnett (6). This theory found successful applications in organic and inorganic chemistry. A homopolar or covalent bond is explained as the linking force engendered by electron sharing between atoms, and each atom contributes one or more electrons to the bond. In an extended lattice or molecule, addition of atoms is continued until all the atoms achieve filled electronic shells by dint of electron sharing. As such carbon having four valence electrons per atom, crystallizes in the diamond lattice with four nearest neighbors. Thereby each carbon atom gets a total of eight shared electrons. Similarly, As, Sb and Bi having five outer electrons per atom crystallize in a lattice with three nearest neighbors, since these elements must share electrons with three neighbors to obtain eight electrons necessary to form a closed shell

configuration. In 1930, Hume-Rothery (7) proposed the (8-N) rule, where N is the number of outer shell electrons, and the factor (8-N) provides the number of nearest neighbors in the lattice. This rule is followed by many elementary covalent crystals in the columns 4, 5, 6 and 7 of the short periodic chart. The covalent bond is limited by the size factor.

Theories of Metallic Bonding and Engel Concepts

Out of several theories proposed for metallic bonding, the following two stand out as significant ones: 1) Electron gas theory and 2) Electron pairing theory.

The electron gas theory has been developed in various stages. In the early stage, the concept of an electron gas in the metallic state as envisaged by Drude (8) and Lorentz (9) was dominant. It was postulated that the outer bonding electrons of the atoms ionize off to generate an "electron gas" which in turn diffuses through a lattice made up of positively charged metal ions as shown in Figure 1 (16). This theory could account for the conductivity of metals but failed to distinguish a conductor from an insulator. Moreover, this could not predict the experimental values of specific heats of the elements.

In an attempt to overcome these limitations, Sommerfeld (10) proposed the principle of quantum mechanics. According to the Sommerfeld theory, the bonding atoms ionize off their outer electrons which assume quantum states common to the entire atom assembly (either a molecule or an extended lattice). It was also postulated that the sum of all the electrons quantized to a very large assembly of ionized atoms known as the electron gas hold the ionized atoms together by electrostatic attraction. The spin interactions were considered extremely small and other

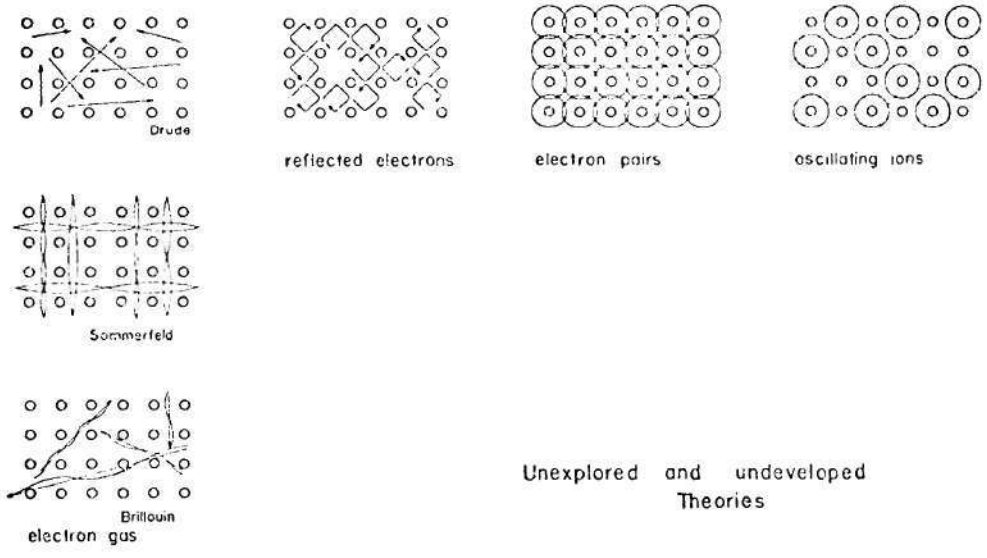

Figure 1. Bonding Mechanisms in Metals.

interactions were ignored. It was assumed that the valence electrons belong to the entire crystal structure, and with the formation of solid phase the energy levels of electrons are rearranged. The Sommerfeld theory further assumed that the electrons move inside a metal at a constant potential as illustrated in Figure 1. A successful explanation for a very low electronic contribution to specific heat is obtained from the Sommerfeld theory, yet this could not explain the difference between a conductor and an insulator. It was equally unable to explain the reason for the magnetic properties in metals and the relationship between typical metallic crystal systems and electron concentration in metals.

In the later stage, Bloch (11) advanced the idea that the valence electrons move in a periodic potential field as demonstrated in Figure 1. The quantized gas theory of Sommerfeld got the modern form on a non-causal basis from Brillouin (12). The various assumptions outlined above provide an outstanding outcome. That is, barring the restrictions imposed by Brillouin zones and metallic lattice boundaries, the electrons have the ability to move in a metal in all directions with corresponding different velocities. The electron gas-Brillouin zone theory accounts nicely for the electrical properties, especially of semiconductor phenomena; provided the electrons are allowed to exhibit various electron masses ranging from positive to negative. However, the theory does not explain many physical properties like melting points, phase diagrams, Young's modulii and alloying behavior etc. Besides there are several direct contradictions with facts such as atomic sizes in solids and the explanation of quantization without a physical cause.

A particle enters a quantum state only when it adopts an orbit in which the

path length is an integer of the mass wave length. This is usually believed to be the cause of quantization. But according to the Brillouin zone theory, the electrons are supposed to move with velocities in essentially straight lines in such a way that the mass wavelength fits into the periodicity of the lattice. This proposition cannot be supported in view of the fact that i) no interaction between an everchanging electrostatic field and mass waves has been known by any evidence, ii) a stationary field and a moving wave cannot react to produce a stabilized movement.

The energy band theory, however, is able to define the difference between conductors and insulators. In a good electrical and thermal conductor like a metal, the electronic energy bands within the Brillouin zones remain partially filled with electrons forming a Fermi surface above which there are empty quantum states and below which all quantum states are filled. Electrons at the Fermi surface can move in an externally applied electrostatic field. In an insulator, however, the energy band in the crystal is completely filled and separated from the next band by a so-called forbidden region of energy, so that the electrons become incapable of undergoing transitions to adjacent quantum states.

Seitz (13), Pauling (14), Mott and Jones (15) and a host of other physicists have given extensive mathematical treatments to the energy band theory. It may be noted here that the mathematical model derived from the gas theory just fits certain experimental observations. In spite of a popular acceptance and support in the world of solid state physics, the band theory has obviously incorporated many non causal concepts, and is, therefore, more a religion than a science.

In accordance with Bohr's atomic model, electrons in a free atom can

occupy different quantum states. Each electronic state in a particular atom is characterized and described by a definite energy and a set of four quantum numbers e.g. n, 1, m_l and m_s. In atoms where only one outer bonding electron per atom is available, the electron will be an s electron in its ground state. Pauling showed by calculation that these s electrons exhibit a symmetrical distribution around the nucleus like hollow balls. A very important characteristic of s, p, d and f electrons is a fixed location of orbit or the electron density pattern. According to the band theory, the fixed electrons in free atoms lose their characteristic identity when the atoms condense to a solid phase; and consequently their specific behavior becomes entirely changed and cannot be calculated without extreme difficulty. The band theory creates another difficulty by its postulate that all the bonding electrons move in different directions within a Brillouin zone. That is, there would be no specific shape of a single bonding electron density if it were really true. Besides, as a result, all the metallic lattices would be something like a close packed lattice, because directional forces cannot be deduced from the gas concept. The model is further unreasonable because it, for example, postulates an energy gap between the second and third p-electrons. This postulate is necessary to explain the insulator properties, but has no physical or chemical justification.

Furthermore, when we examine the atomic size of the inert gas atoms and adjacent alkali metal atoms (Figures 5, 6 and 7; Chapter II), the fallacy of gas theory is easily exposed. If the electron gas theory were true, consequent upon ionization of metal atoms, the outer shells of sodium ions should be expected to

touch each other. And as such the metallic Na atoms should be expected to be smaller than the previous inert gas atoms Ne, or the sodium ions should be about the same size as atoms in metallic Na. But the reverse is true. And it is known that all metallic ions are much smaller than the same atoms in the metallic state.

Engel (16) suggested the reflected electron theory (Figure 1) in an attempt to surmount this difficulty. According to this, the electrons get reflected from the lattice planes and adopt orbits within atom tetrahedrons and atom octohedrons such that the path length becomes an integer of electron mass wavelength. This theory was not accepted since it was believed that it envisaged the electrons to enter quantum states on a potential top. As a matter of fact, in case of gas theory the electrons do the same more explicitly.

The aforesaid inadequacies and haziness of the electron gas theory warranted the necessity of a clear picture of bonding mechanism in metals on a rather causal basis.

The electron pairing theory was introduced by G. N. Lewis (4, 5). This theory is essentially based on the concept of stability of filled electronic shell as established by spectroscopic data (Hund's rule) (24). Subsequently Heisenberg (17) in 1925 and Schrödinger (18) in 1926 applied the concept of quantum mechanics to the electron pairing theory in order to explain the covalent bonds. Heitler and London (25) and Hartree (26) provided a better quantitative basis for the calculation of bonding of electron pairs. Although supported by many experimental facts from spectroscopy, organic and inorganic chemistry, the Hume-Rothery (8-N) rule, atomic distances etc., the pairing theory is still less understood and as such less

investigated in comparison to the gas theory. In 1949 Engel (19) for the first time extended the concept of electron pairing to account for the metallic covalent bonding. Engel further applied his ideas to explain the metallic properties such as cohesive energy, melting points, boiling points, elastic properties, activation energies, phase diagrams, electrical properties, etc. by postulating that the metallic lattices are electron concentration controlled. Brewer (20) much later recognized the virtue of the Engel concepts and used them extensively in many areas especially in prediction of high temperature metallic phase diagrams.

As pointed out earlier, the covalent bonds occur due to the interatomic binding forces generated by the sharing of electron pairs. In other words, when lattices or molecules are formed, all the electrons which hitherto were unpaired in the free atoms become stably paired. All electrons remain in quantum states around one atom only, preferably the mother atom to form a homopolar bond. Besides, according to the electron pairing theory, the bonding electrons always retain their specific identity or character e.g. size and shape of orbit and energy level in forming bonds. Owing to the liberation of energy by (external) pairing, the initially fixed electronic energy levels appear lower which may be different for s, p or d electrons. Whereas in case of the gas theory, the electrons enter new quantum states and get quantized to the whole multiatomic complex by itself. Further, it is argued that the energy levels of s, p and d electrons on the Fermi surface rather combine together to form a band of energies.

The Engel concepts are essentially based on the generally accepted view that the free atom possesses a well defined pattern of quantum states. Engel (19, 16)

introduced the idea that these quantum states are basically rigid. Through a new particle model he introduces a new force which releases energy when particles occupying quantum states pair. He considers it almost absurd that the electronic quantum states linked to many ions can exist as ordinary moving electrons, since no quantum state can develop on potential maxima or ridges. Also no quantum state can be fixed when related to many atoms constantly changing distance due to heat vibrations. For eventual bonding between the atoms, the electrons have got to jump from one quantum state to another. More bonding electrons may generate due to electron jump and some electrons may remain in excited states forming more bonds. Engel (19, 16) postulates that the atomic bonding takes place due to the formation of electron pairs. Engel (21, 16) also proposed a cause-effect related particle model to account for the physical forces and mechanisms responsible for the quantization and pairing of electrons. It is postulated here that all the particles are built up of energy waves propagating with the velocity of light in a fixed frame of reference or a so-called wave carrier or ether. According to this model, the moving particles have been considered as elongated particles or long snake-like structures exhibiting wave properties rather than as points or balls.

Recognizing the different effects of bonding electrons in s, p, d and f states, Engel (19, 22) advanced the electron oscillator theory, according to which the electrons in quantum states behave as rigid oscillators. Founding on this while extending the Hume-Ruthery (18 N) rule, Engel (19, 23) proposed the famous "Engel Correlations" in which the metallic lattices have been viewed as electron

concentration phases. In this respect, Engel postulates that the metallic lattices are controlled by the number of outer bonding electrons per atom. As such, the body centered cubic lattice is a one electron per atom phase, the hexagonal close packed lattice is a two electrons per atom phase and the face centered cubic lattice is a three electrons per atom phase. In this light, an examination of the transition metals proves most interesting. In transition metals, all unpaired d-electrons participate in the bonding process, but don't control the lattice type--which is solely a function of the number of outer (s+p) bonding electrons (19, 23).

The Engel Correlations successfully account for the distribution of lattices over the periodic chart on a causal basis. The lattices of metallic elements in different periods can be determined by the concentration of outer bonding electrons. These correlations can also be applied in the reverse order, such that the electron concentrations can be determined from the lattices. The Engel concept of bonding can be used to explain the causal relationship between the bonding mechanism and the thermodynamic, electrical and magnetic properties of the metals (especially for the transition metals). Engel's theory has several other useful and important applications in explaining the atomic size, the inorganic structural rules, physical properties, compound formation, alloying behavior and prediction of phase diagrams etc.

We will examine here the thermodynamic properties of the elements in the periodic table as explained by the Engel Correlations. As demonstrated in Figures 2, 3 and 4, we can find that the peaks of melting point curves appear in the middle of the transition elements, sixth column and in the middle of the normal elements

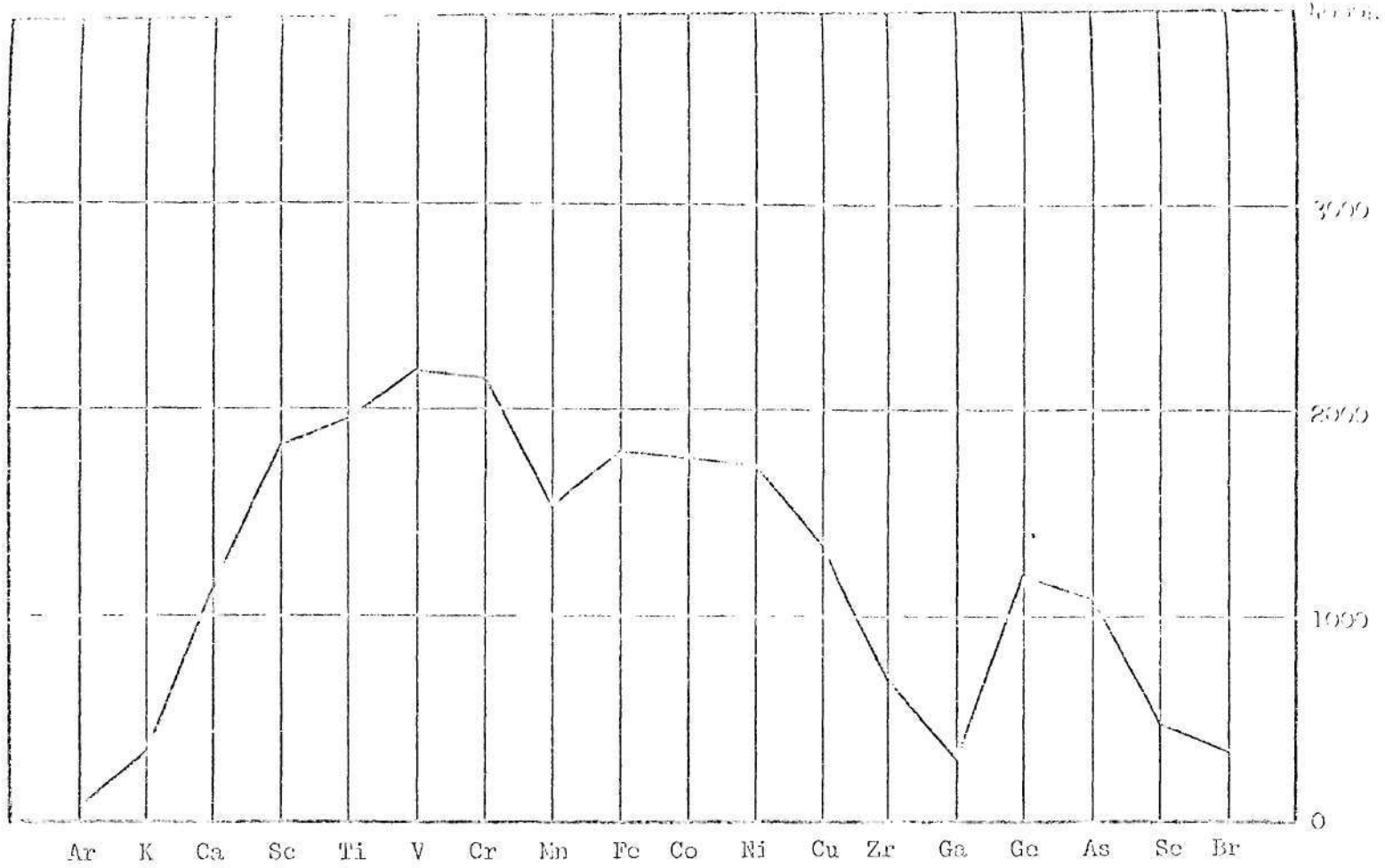

Figure 2. Melting Point of the Fourth Period Elements.

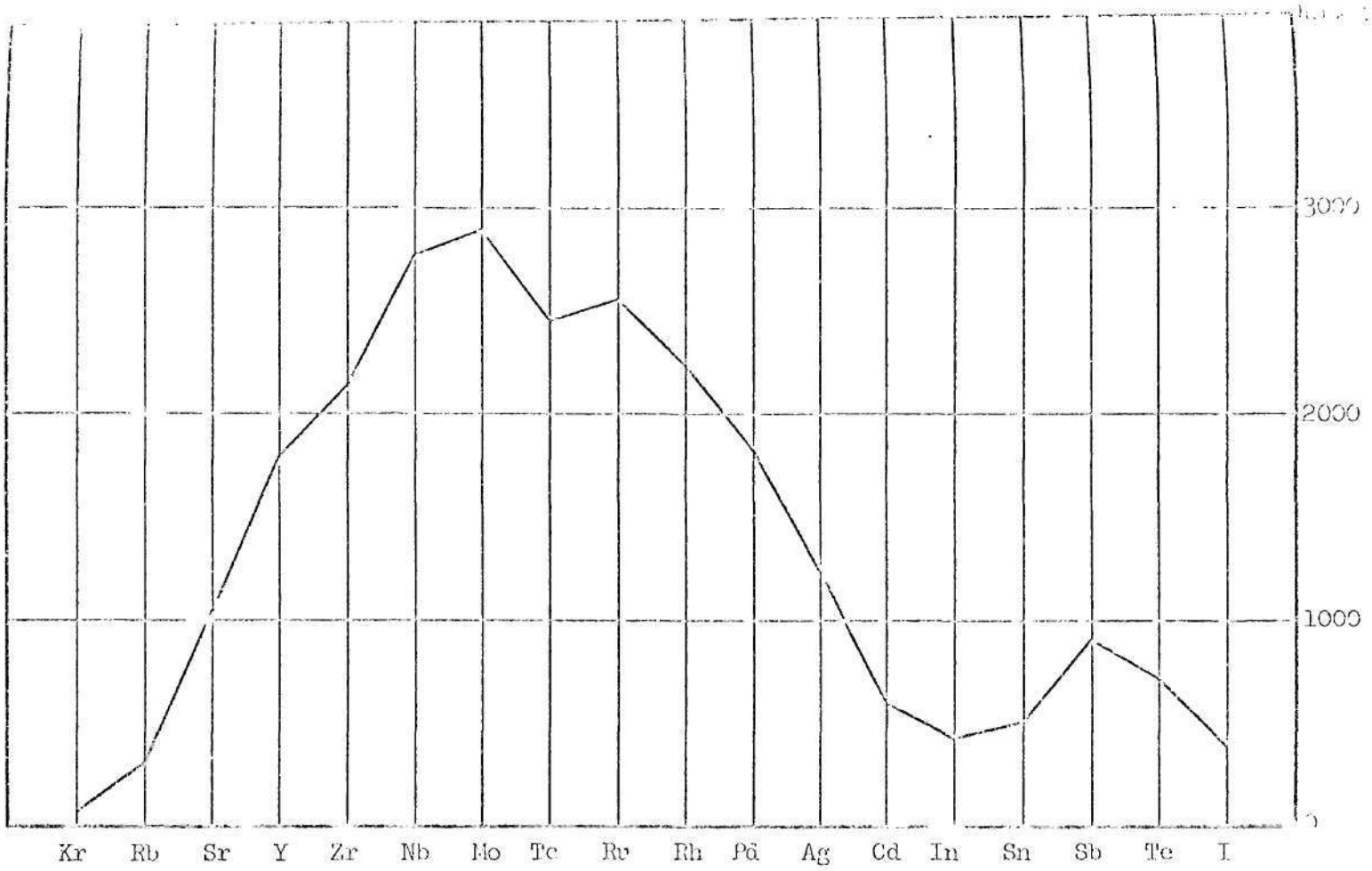

Figure 3. Melting Point of the Fifth Period Elements.

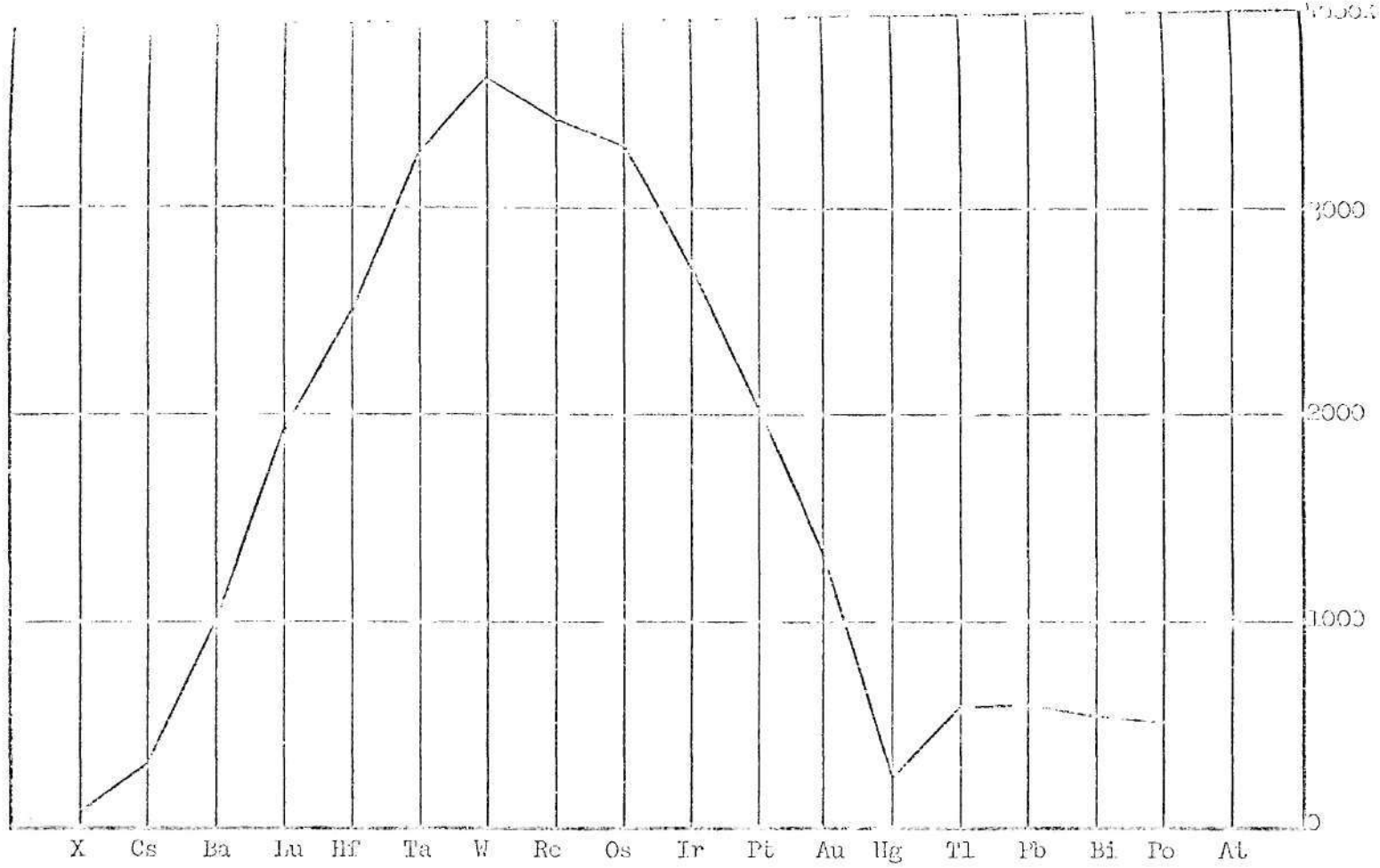

Figure 4. Melting Point of the Sixth Period Elements.

and fourteenth column. The sixth column elements with b.c.c. lattices have one outer electron per atom. Thus in the sixth column elements, the d-electron shells remain half filled and all the five d-electrons are unpaired and participate in bonding. Since five unpaired d-electrons is the highest number possible, highest bonding strength and melting point should be expected in the sixth column. In the fourteenth column elements having no d-electrons, four outer electrons per atom take part in bonding. The peaks in melting point and bonding strength in normal elements again appear in the fourteenth column, as four covalent bonds in normal elements is the highest number obtainable.

According to the gas theory, the upper energy levels have been assumed to be the same for s, p and d electrons. According to the Engel's postulates, the energy levels and orbit sizes of bonding electrons should differ. As will be seen in the following chapters, the present investigation has been undertaken to verify the Engel theory. It is hoped that compression or tension would provide a measurable thermal effect as predicted by the Engel theory.

CHAPTER II

THEORETICAL BACKGROUND

As defined earlier, the purpose and approach of this investigation will be described in this chapter on the basis of the electron pairing theory and Engel concepts.

It is of paramount importance to note the Engel postulate that the bonding electrons maintain their characteristic size and shape of orbit and energy level in bonded condition (solid state) as well as in free atom. Besides owing to the energy released by electron pairing, the originally fixed electronic energy levels appear lower. In transition metals, the outer (s+p) electrons make bonds selectively with (s+p) electrons and d electrons give the strongest bond with other d electrons. That is, the half-filled d shell (with five unpaired d electrons) provides the maximum bonding strength. In pure transition elements, an equilibrium exists between the concentration of s+p electrons and d electrons. This equilibrium is influenced by average nuclear charge, temperature and pressure etc. According to the Engel theory, in such metals, both s+p and d electrons take part in atomic bonding. It should be borne in mind that the outer (s+p) electrons are lattice controlling, whereas d electrons are not. This is related to the fact that the bonding energy unleashed per d electron bond is about twice that released by formation of outer electron bond.

In the present investigation, it has been considered reasonable to assume

that the interatomic distance in solid state is controlled by the sizes of the s+p electron orbits as well as the d electron orbits. In this connexion, a study of the atomic distance variations over the fourth, fifth and sixth periods will be inevitable (Figures 5, 6 and 7) (27). In these figures, the upper curves represent a calculated atomic distance assuming that bonding is controlled by outer (s+p) electrons only; the lower curves indicate a calculated atomic distance assuming only inner d electrons determining the atomic distances. The thick line curves give the actual atomic distance as measured by X-rays. We find invariably a dip in the middle of the transition elements i.e. smallest atomic size. In other words, a maximum of five-d bonding is dominant here and the atomic size or the interatomic distance becomes minimum. In the transition elements, it appears that a kind of stress operates between (s+p) and d electrons; d electrons pulling down and s+p electrons pulling up. As a result, the s+p electron shell finds itself in a state of compression by drawing energy from the d electron shell.

For the calculation of the upper curves, the assumption has been made that the atomic distance contracts with increasing nuclear charge. For example, Rb being the first element in the fifth period (Figure 6), will have only one s electron in the fifth shell and no d electrons in the fourth shell. For the upper curve, the calculated values of each element in the fifth period are given by the relationship $\frac{Rs.37}{Z}$, where Rs is the atomic distance between Rb atoms in solid state, 37 is the atomic number of Rb and Z is the atomic number of the particular element. Similarly the values for the lower curve corresponding to each element in the fifth period is obtained from the relationship $\frac{Rs.37}{Z} \cdot \frac{4^2}{5^2}$, where 4 and 5 are the principal

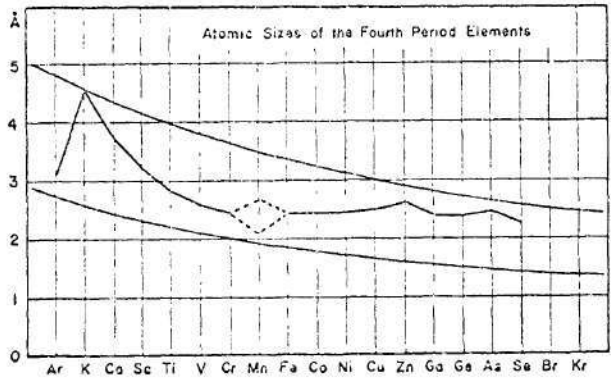

Figure 5. Atomic Distance of the Fourth Period Elements.

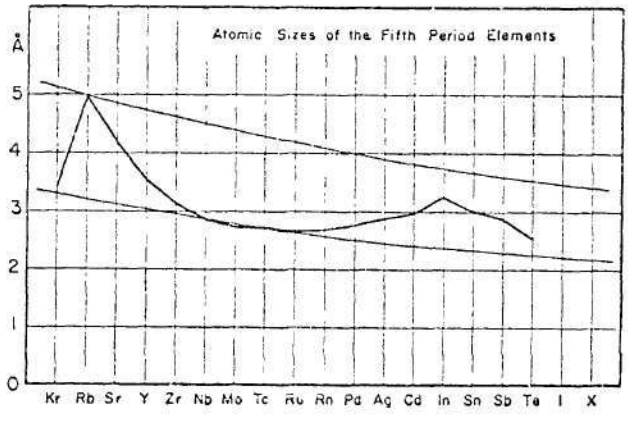

Figure 6. Atomic Distance of the Fifth Period Elements.

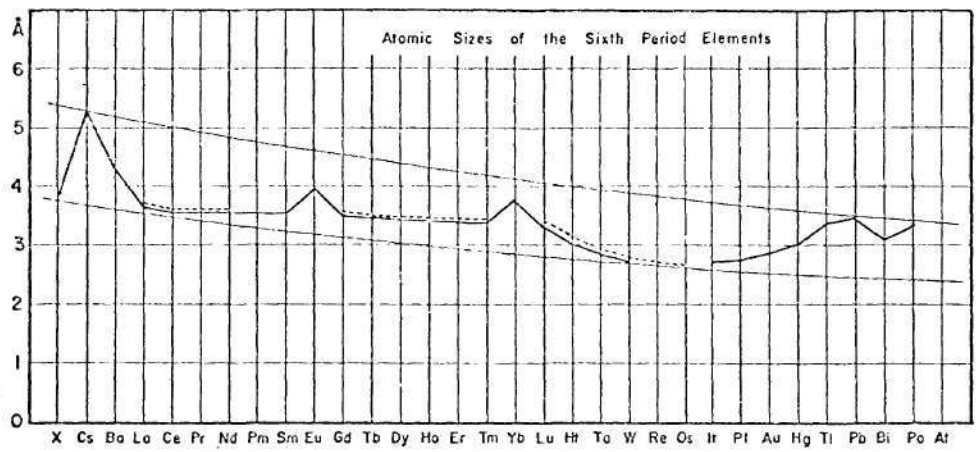

Figure 7. Atomic Distance of the Sixth Period Elements.

quantum numbers for the d electrons in the fourth shell and s electrons in the fifth shell respectively. The upper and lower curves in the fourth and sixth periods (Figures 5 and 7) are plotted on the basis of similar computations.

In the first chapter, it was derived from the Engel postulate that the highest bonding strength shows up in column six elements (Cr, Mo and W) having one outer s electron and five d bonding electrons. As is evident from Figures 5, 6, and 7, in case of Cr, Mo and W the actual atomic distances are close to the lower plots, which have been constructed considering that only d electrons were responsible for the bonding process. However, a considerable variation in actual atomic distances could be noted for the remaining elements of these three periods. Most atomic distances are located in the region between the upper and lower plots in each period. In light of the above, it would seem reasonable to state that the atomic distances of alkali metals K, Rb and Cs (column one) are determined only by s electron bonding; and that of Cr, Mo and W (column six) are dominated by d electron bonding. The atomic distances of the elements between the two extremes are influenced by both outer and inner electrons. As such the actual interatomic distances should essentially depend on the number of s+p as well as d electrons. It will be reasonable to assume that the electron transfer between the outer and inner shells is determined by the following factors: (i) the electronic structure of free atoms (ii) the promotion energy necessary for the movement of electrons between the outer and inner shells and (iii) the bonding energy.

The atomic distance and at times the crystal structure are affected by thermal energy; the transition elements Ti, Zr and Hf (column four) exhibit

allotropic transformations. For instance, the low temperature α phase of Ti (H.C.P.) changes to the high temperature β phase of Ti(B.C.C.), as one electron drops from s+p shell to the 3rd subgroup due to thermal vibrations. Because heat energy can expand a metal and can influence its electronic structure resulting in allotropic transformations, it is believed, that an application of stress (one axial) or pressure (three axial) can also alter the electronic structure of a metal. Upon stressing or compression, the difference in shell size between the outer (s+p) and d electrons or the promotion energy between the outer and inner shells should give rise to the electronic movements between these shells. In transition metals, as a rule, the d bonding will be favored and the s+p bonding will be unstable under pressure.

The electron movement between the outer and inner shells becomes quite unlikely and increasingly difficult, when a high promotion energy between the two shells is needed for such movement. The high promotion energy region occurs in extreme cases where the actual atomic distances are very close to the upper or lower curves. For example (Figures 5, 6 and 7), the atomic distances of Cr, Mo and W are considerably close to the lower curves giving a pure d electron bonding, and that of K, Rb and Cs almost touch the upper curves, representing a pure s electron bonding. Fastest electron movements should, therefore, be expected in case of elements whose interatomic distances are placed between the upper and lower curves and where the promotion energy required for electron movement between the two shells is the least. That is, under pressure or stress, a better propensity for electron movement could be anticipated in column four elements

(Ti, Zr and Hf) of lower promotion energy region than in column six elements (Cr, Mo and W) which belong to the higher promotion energy region and where the atomic size variation with increasing electron addition matters little.

When a metal is stressed or compressed, its atomic distance is changed influencing the lattice vibrations. As such the electronic structure is also changed. According to the electron gas theory, the lattice is expected to cool down in compression, since the electrons absorb energy. But to the contrary, the lattice heats up. When the atoms are brought closer to each other, the velocities of electrons in gaseous quantum states increase. In the compressed material the electrons should move faster due to their shorter wavelengths; and as such the kinetic energy of the electrons goes up. It is known that the kinetic energy of electrons in quantum states originate from potential energy between the charges (in free atoms), half of which emits as light. In compression, the acceleration of electrons should cause the electrons to absorb energy according to the gas theory. However, a calculation for energy absorbed by the electron gas in compressing Na, as illustrated in Appendix A, shows a clear disagreement of the electron gas theory with the observed facts.

According to the Engel concept, it is expected that a suitably designed adiabatic heat experiment could provide a means to measure the electronic movement between the outer and inner shells due to tension or compression. This paper will be confined to the investigation of adiabatic heat of compression of many elements with a special interest in metals. The internal energy change of the elements because of compression can be determined in the following way:

Change of Internal Energy = Heat Output - Work Input.

(The heat output is the temperature increase due to compression multiplied by the specific heat of the material.) The electron movements between the outer and inner energy levels by virtue of promotion energy should be measurable as a part of the internal energy change. The trend of electron movements could also be obtained by a study of promotion energies between the different energy levels. It is hoped that this investigation will help provide a causal understanding of bonding mechanism in metals.

CHAPTER III

EXPERIMENTAL WORK

General Principle

The experiment is designed to investigate the thermoelastic effects of metals in order to indicate the electron movements between its outer and inner shells (in metals) associated with compression. This indication could be found in the adiabatic heat of compression.

A dynamic hydrostatic pressure device was considered suitable to accomplish the desired end. Through this device a cyclic three-axial stress or pressure could be applied providing an adiabatic condition. For this purpose, a punch press machine with a frequency of 4 c.p.s. and a throw of 1 1/2" was employed in conjunction with a hydrostatic pressure vessel. The frequency of cyclic compression was optimum for the prevention of heat exchange with the surroundings and for easy recording. Figure 8 shows a schematic sketch of the principal parts of the pressure generating vessel and insulated heat output system. Figures 9-11 are the photographs exhibiting the arrangements of punch press machine, pressure vessel and electrical gadgetry (Figure 9a), a closeup of pressure vessel, valve and pressure cell (Figure 9b), specimen holders and specimen (Figure 10), and the details of insulated heat output system (Figure 11). The pressure variation is measured by a pressure cell attached to the pressure vessel. The thermocouples placed on the specimen measure the temperature increase due to elastic compression

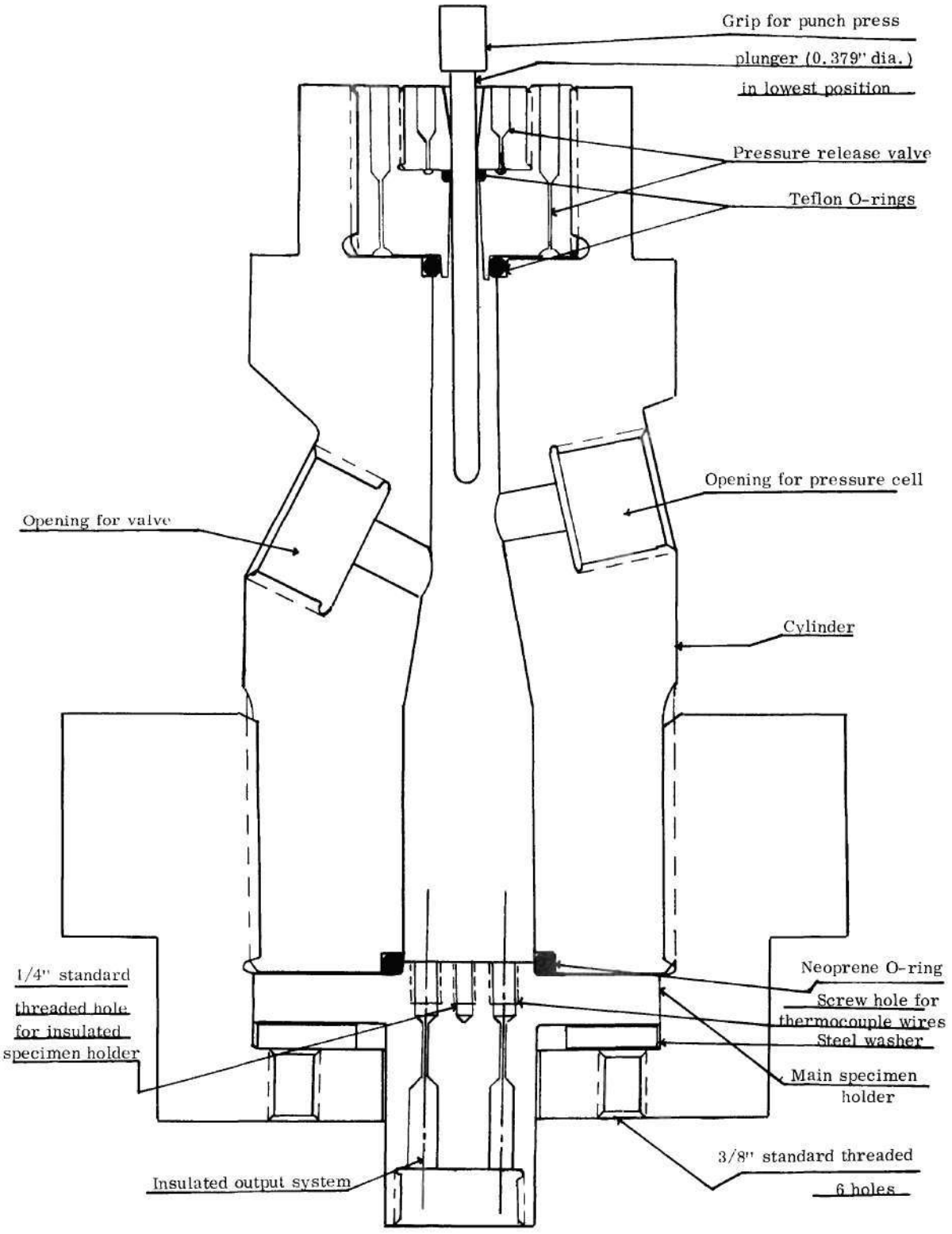

Figure 8. Setup for Pressure Vessel & Heat Output Measurement.

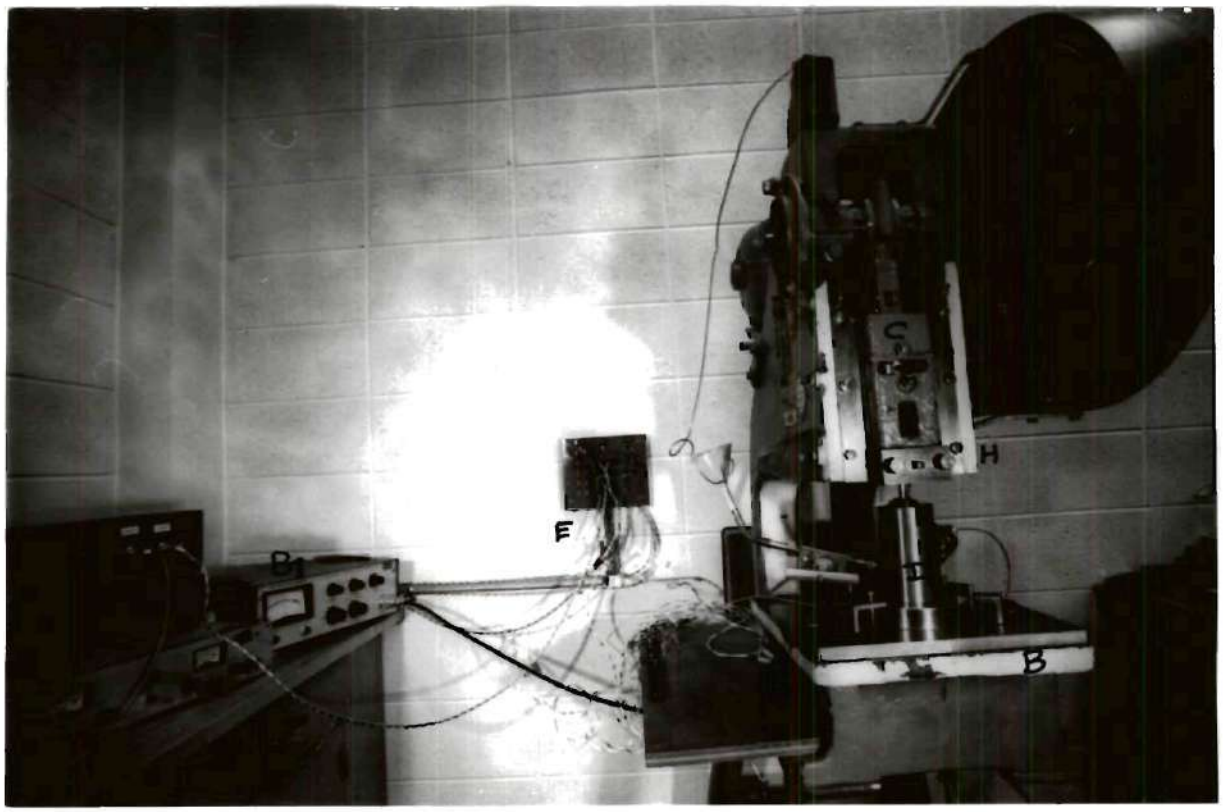

A. Temperature calibration box

B1. Amplifier

C. Punch press machine

D. Pressure vessel

E. Electrical connexions

Figure 9a. Arrangements of Punch Press Machine,

Pressure Vessel and Electrical Gadgetry.

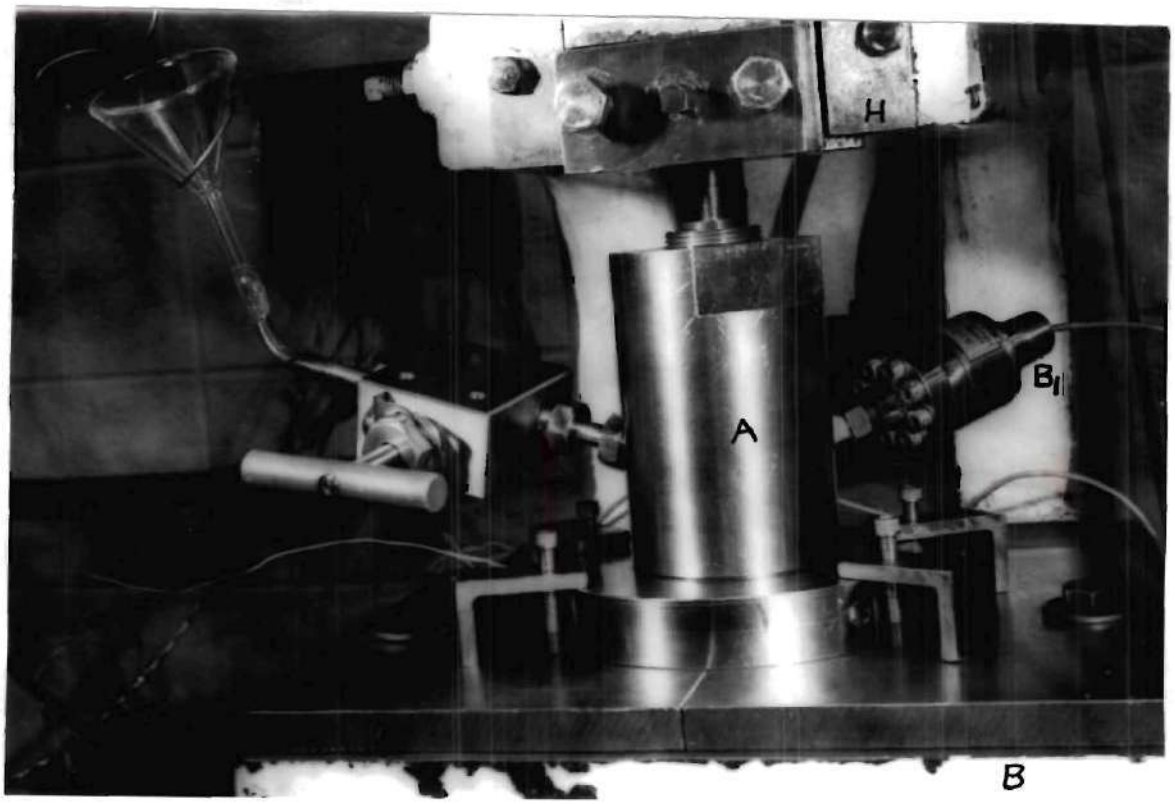

A. Pressure vessel

B1. Pressure cell

C. Valve

D. Plunger

Figure 9b. A Closeup of Pressure Vessel,

Valve and Pressure Cell.

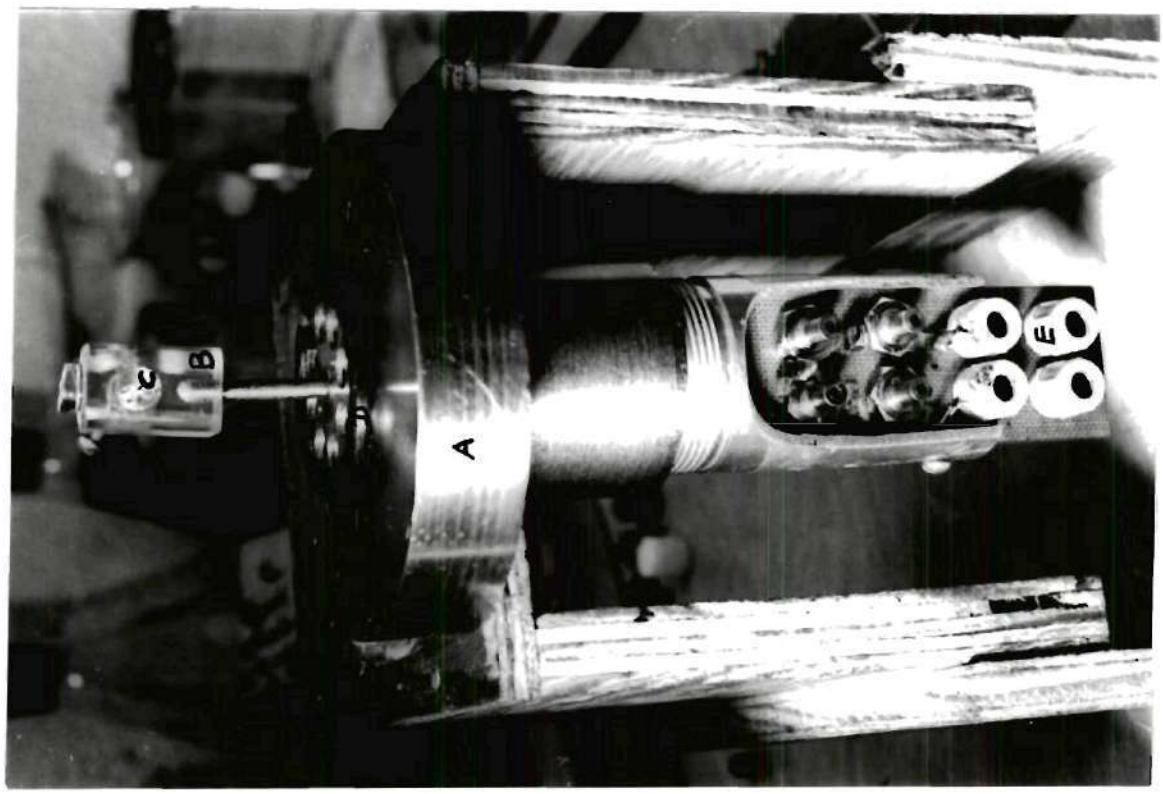

A. Main specimen holder

B. Specimen holder

C. Specimen

D. Neoprene O-ring

E. Thermocouple cold junctions

Figure 10. Specimen Holders and Specimen.

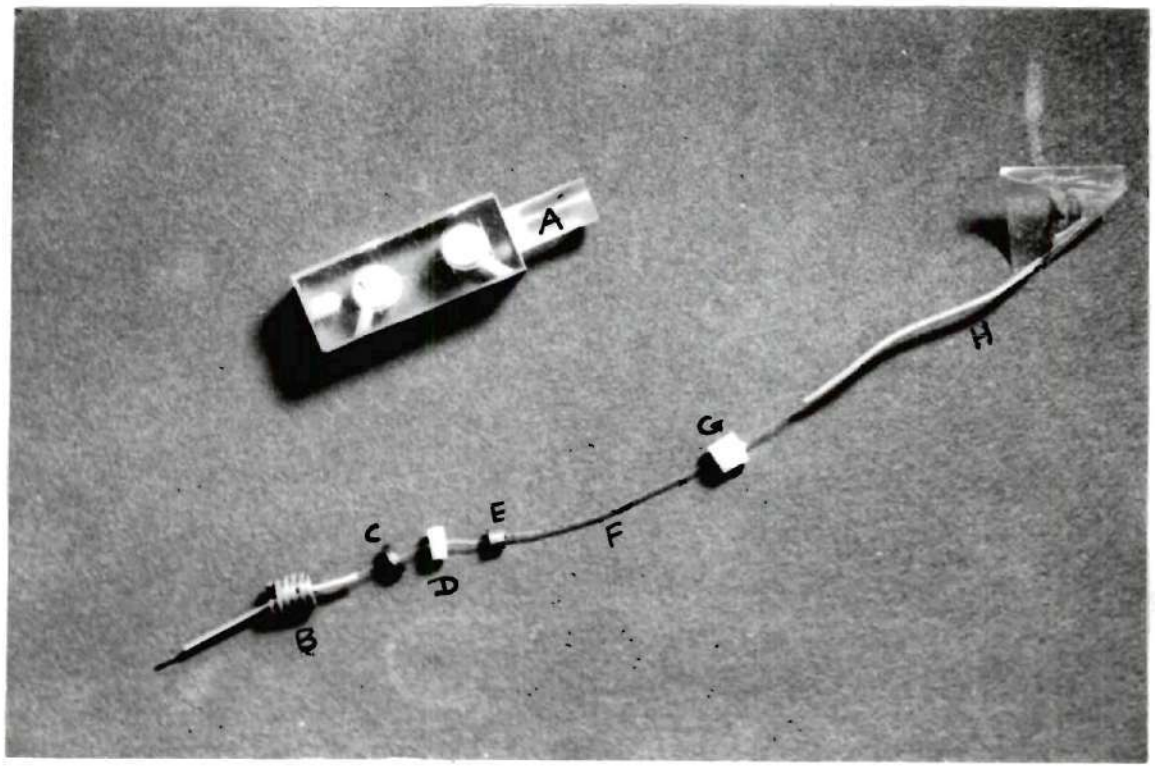

A. Double specimen holder

B. Screw

C. Steel washer

D. Teflon disc

E. Disc (thermocouple material)

F. Thermocouple wire

G. Teflon cup

H. Insulating tube

Figure 11. Details of Insulated Heat Output System.

under adiabatic condition.

Instrumentation

The layout diagram (Figure 12) shows the basic instruments used in our experiment. An oscillograph was invariably employed to measure the two variables, temperature and pressure simultaneously in terms of their corresponding electromotive force variations. In order to measure the temperature variations, the thermocouples on the specimen send electrical signals to a visicorder via an amplifier wherein these are recorded on the photographic paper as changes in thermal e.m.f. Similarly the pressure variations were measured as potential changes from the Weatstone bridge of a pressure cell connected to the pressure vessel and recorded on the same visicorder through a different channel. Because the temperature variations due to compression were too small to be recorded directly, an amplifier was used before recording on the visicorder. A precision potentiometer was also employed to standardize the D.C. power supply to the pressure cell and for the calibration of temperature and pressure measuring devices. A brief description of the important instruments used will be given below.

As described above, for direct recording of temperature and pressure variations, a rack mounted type Honeywell model 1508 Visicorder was used. The writing frequency of the oscillograph can be varied from 0 to 5,000 c.p.s. depending on the type of miniature galvanometer used. Out of several electromagnetic damped galvanometers, M40-350A was chosen for temperature measurement, and M100-350 for pressure measurement. The galvanometer M40-350A has a flat

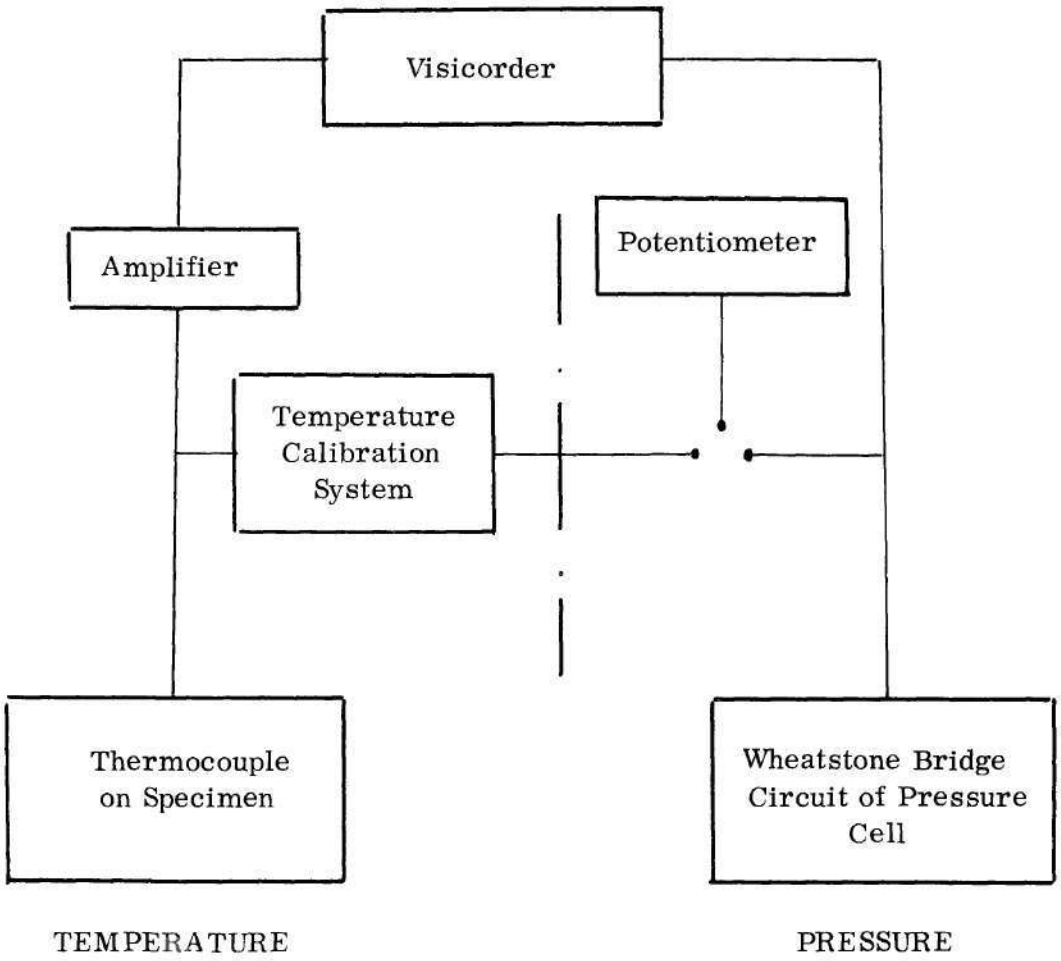

Figure 12. Layout of Principal Instruments.

frequency response of 0-24 c.p.s. and voltage sensitivity 0.250 mv/in, whereas the galvanometer M 100-350 has 0-60 c.p.s. and 0.529 mv/in respectively. (It has been shown in Appendix C that the accurate value of the voltage sensitivity of galvanometer M 100-350 is 0.529 mv/in and not 0.432 mv/in as given in the visicorder operating manual.)

Keithly model 148 Nanovoltmeter (Figure 9) was used to amplify the measured thermal e.m.f. before recording on visicorder, since the corresponding temperature variation involved was very small. For our experimental purpose, the amplification of 0.1 millivolt range was fairly suitable and produced no noise. The amplifier can also be operated by a battery. This assured a complete isolation of A.C. power line, as such eliminating grounding difficulties, noise and other interferences due to A.C.

For pressure variation measurement, BLH type DHR pressure cell was employed. The cell has a capacity of 20,000 p.s.i.g. and can take a load of 20 V. It can translate changes in fluid pressure into corresponding changes in output signal voltage (in mv). In this pressure cell, bonded foil-type SR-4 Strain Gages, especially designed for diaphragm strain measurements are used, and are connected in a Wheatstone bridge circuit. Any variation of fluid pressure displaces the pressure sensing element or the diaphragm, which in turn causes the strain gages to change resistance slightly. The bridge balance is upset due to this change in resistance and produces a change in output signal which varies proportionally to the pressure change on the diaphragm.

Leeds Northrup 7553 Type K-3 Universal Potentiometer was used in order

to maintain and check a constant D.C supply on the pressure cell and for the calibration of temperature and pressure measuring circuits. This potentiometer can measure only from 0 to 1.6110 volts. And since it was required to apply 5 V on the pressure cell, a special device as shown in Figure 14 was adopted to measure beyond 1.611 V. According to this, the unknown e.m.f. is connected across a series of precision resistors and a definite known fraction of total unknown e.m.f. is applied to the potentionmeter. By multiplying the potentiometer reading by the factor 5, the total unknown e.m.f. on the pressure cell is easily evaluated. As illustrated in Figure 14, the definite known fraction of unknown e.m.f. across FG is about 1 V; as such the total unknown e.m.f. across EG turns out to be approximately 5 V. This is also roughly checked from the reading of voltmeter incorporated in the visicorder.

Device for Temperature Measurement and Calibration

For temperature measurement, a wide range of methods was adopted to fix thermocouples on the specimens. Small cylindrical (usually of 1/4" dia. and 1/2" length) or block-type specimens of elements of varying sizes were prepared depending on the size, shape and weldability of the available material. Correspondingly, the specimen holders differed in design and were made in plexiglas and phenolic. But all had a pair of small screws to tighten the specimens. In case of a B.C.C. metal, the thermocouple wires were mechanically punched into small grooves worked out on the face of the cylindrical specimen fitted in an especially designed vice before putting it into the holder. The holes for wires were closefit for a good thermal contact but not too close fit to have any strain on it

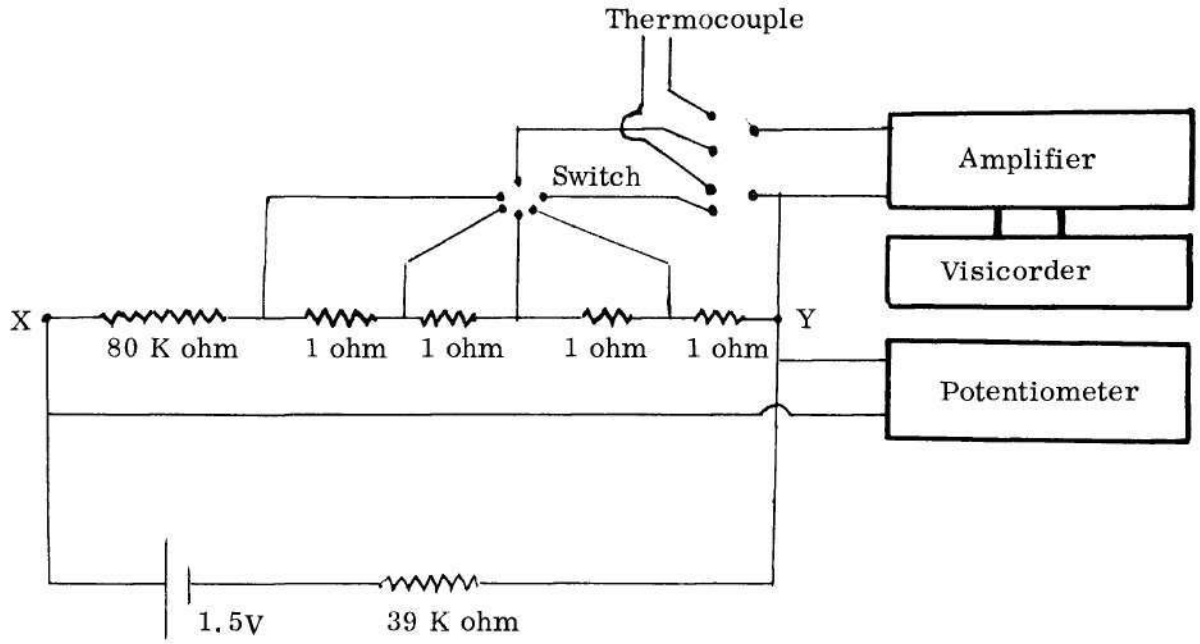

Figure 13. Circuit Diagram for Temperature Calibration.

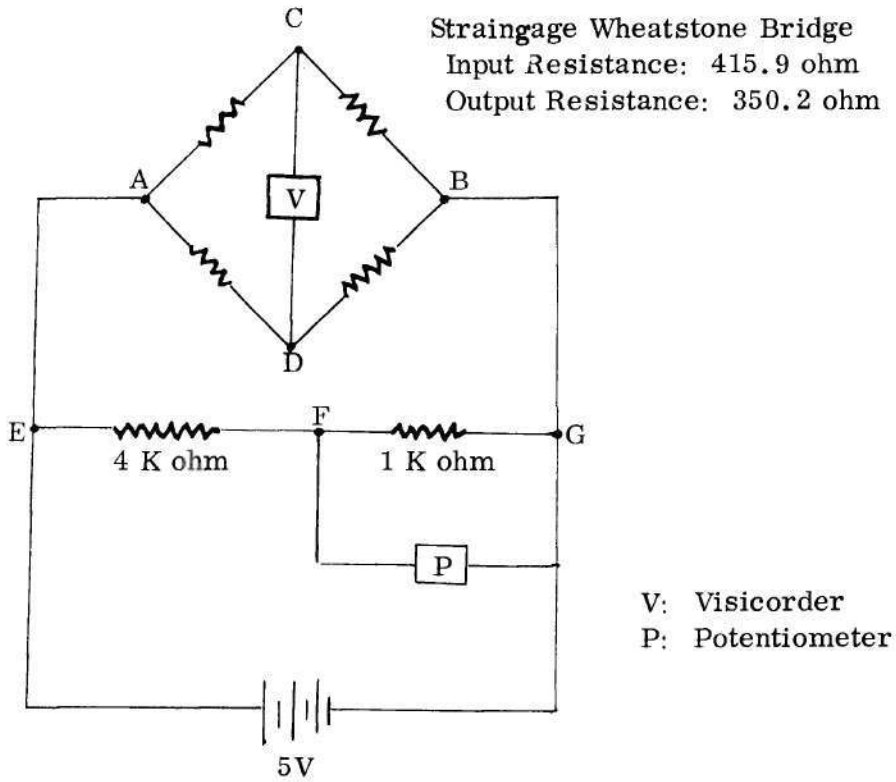

Figure 14. Pressure Cell Circuit in Conjunction with a Device for Voltage Multiplication Factor.

arising from the viscosity of the transmitting medium. On round surface of cylindrical and flat surface of block-type speciments, the thermocouple wires were resistance welded by a spot welder. A good thermal contact of thermocouples was nsured by a checking device. The thermocouple wires were just stuck in on the block--type specimens of sulfur and alkali metals Li, Na, K and Rb. A special mild steel cup was employed to hold Hg and Cs (melting point 28^{o}C). Insulated thermocouple wires were again stuck into the metal. The experiment on Cs was performed at different temperatures ranging from 15-30^{o}C. Low temperature of the metal was attained by covering parts of the pressure vessel with dry ice, and a hair dryer was used to raise the temperature. Special care was taken to prevent the oxidation of the alkali metals and other susceptible metals during handling and experimenting. A suitable e.m.f. range was provided by chromel-alumel thermocouples. Since wires of 0.002" dia. did not give reproducible results in most cases, the wires used were of 0.0125" dia. except in case of W and Te, where 0.002" dia. wires were employed. The 0.002" dia. thermocouple wires were spot welded on W specimen, whereas on Te specimen these were pressed in by a hot solder gun. On Ge specimen, 0.0125" dia. wires were fixed rigidly in fine drilled holes. Since it was not possible to weld or punch thermocouple wires on Si, the 0.0125" dia. wires were tightly held between the flat surfaces of two small pieces of Si (p--type) in the specimen holder. This gave a good thermal contact. In general, the two thermocouple wires were affixed to the specimens near each other, but not touching each other. In case of Si and S, however, the two ends of the wires were prewelded before affixing to the specimens.

Throughout the thermocouple wires were carefully insulated with spaghetti plastic tubes. Figures 10 and 11 show the specimen, specimen holders and insulated heat output system. In order to avoid thermal noise while measuring small thermal e.m.f.s., electrically shielded copper cable and clamps were used to connect the specimen thermocouple and the amplifier. Usually two pairs of thermocouples were employed in order to obtain repetitive and reproducible results for the same element. Cold junction correction was not necessary, since only temperature variation and not the absolute temperature was sought to be measured.

Figure 13 illustrates a special electrical circuit for temperature calibration, since the conventional temperature calibration devices are of no use in our case, where very low temperature variations are involved. The calibration circuit consists of a series of 80K ohm and four standard 1 ohm resistors connected to a D.C. source. A four-step switch was connected to the group of four 1 ohm resistors. The universal potentiometer could measure the potential difference between X and Y accorately up to four decimal places. In this way, an accurate potential drop across the group of four 1 ohm resistors was represented as four-step deflection on the visicorder photographic paper. The details of the calibration calculations are given in Appendix B. Figure 16 shows a photograph of a typical curve of temperature calibration, where 1 cm of temperature deflection equals to 0.1068 V.

Device for Pressure Measurement and Calibration

The pressure system is composed of an especially designed pressure vessel connected to a punch press machine. A pressure cell is attached to the

pressure vessel. Depending on the pressure tightness and absence of air in the vessel, a pressure up to 2,780 p.s.i.g. could be developed. A purely hydrostatic pressure is necessary for a uniform three-dimensional stress on the specimen. The experiments with glycerine gave non-consistent and erratic results, although it developed a very high pressure because of its quite low compressibility. The deflections obtained on visicorder due to temperature and pressure variations were rather abnormal with flat ends. At pressure levels generated by glycerine, thermo-elastic effect seems to lose its linearity with pressure. As such a lube oil with a low compressibility to generate a reasonably high pressure was used which gave normal deflections and consistent results. The cylinder of the pressure vessel employed has a capacity of 100 cc. The contrivance for the generation and transmission of hydrostatic pressure on the adiabatically insulated specimen is shown in Figures 8 and 9. The pressure vessel parts are made of ferritic stainless steel except the plunger which is a hardened drill rod. The pressure technique required a leakproof sealing extensively. The plunger or piston of pressure vessel was connected to the head (H) of the punch press, and the rest of the vessel was rigidly fixed on the base (B) of the machine. About complete removal of trapped air from the pressure vessel and pressure tightness were the prerequisites for good experimental results. As the head of punch press moves up and down, the fluid pressure generates by the displacement of the piston, and in this manner the specimen placed in the holder inside the vessel is compressed and decompressed.

The pressure variation was measured by BLH type DHR pressure cell and was recorded on the visicorder. The universal potentiometer checked a constant

D.C. supply of 5 V on the pressure cell before and after each experiment. The working of these instruments has been described under "instrumentation" above.

Figure 14 shows the circuit for pressure measurement. The circuit also shows how 5 V on the pressure cell can be measured by the potentiometer. In Appendix C the detailed computations of pressure calibration have been provided. It was found that 1 cm of deflection corresponded to 278 p.s.i.g. pressure.

Preparation of Specimen

In most cases, depending on the size, shape and weldability of available material, specimens were made in the form of small cylinders (usually of 1/4" dia. and 1/2" length) or blocks of varying dimensions. The thermocouple wires were of 0.0125" in diameter, thus the mass of the specimen was always large compared to the mass of the thermocouple. In order to determine the influence of deformation on the thermoelastic effect, cold worked specimens of Fe and Cu were annealed at 1200^{o}F for one hour. The temperature variations of annealed specimens due to the elastic compression were compared with those of the corresponding cold worked specimens. The deformed and annealed Cu and Fe showed the same effect, when the hardness was reduced from RB 80 to RB 38 and from RB 86 to RB 46 respectively. This result permitted the use of either cold worked or heat-treated material. The influence of different pressure levels (generated by oil as pressure generating medium) on the temperature variation was checked. With specimens much larger in mass than that of thermocouples, the ratio of temperature variation to pressure for different pressure levels was found to be practically constant. This was also verified when specimens of Fe and Ti of different

diameters were tested at varying pressure levels. These experiments showed that the diameter of the specimen exercises no influence on the results.

CHAPTER IV

DISCUSSION OF RESULTS

Errors in Measurement

In preliminary investigations, some experiments were carried out with a single wire loop in lubricating oil as pressure generating medium. The loop generated an unexpected electrical voltage which passed through zero at the pressure extremes as shown in Figure 15. No such effect would be expected since the wire and leads were of the same material and, therefore, no thermocouple effect was possible. Further investigations with copper, chromel and alumel wire loops showed the same pressure effect but of varying magnitude. We believe that this pressure effect is caused by a pressure gradient developed in teflon discs which sit at the bottom of the main specimen holder. Figure 15 shows that the pressure effect is due to a differential buildup of pressure in the leads to the loop. In view of the influence of pressure effect on our temperature measurements, the static device for pressure application was abandoned. Subsequently the dynamic method was adopted where this effect could be cancelled out. In this case the pressure and thermocouple measurements are done at the pressure peaks (Figure 15) where the wire lead anomaly is zero.

The systematic error in temperature measurement due to the low frequency overshoot of the amplifier is 1.7% for all the amplification ranges. The noise is negligible for 0.1 mv range most often used. Several sources of random

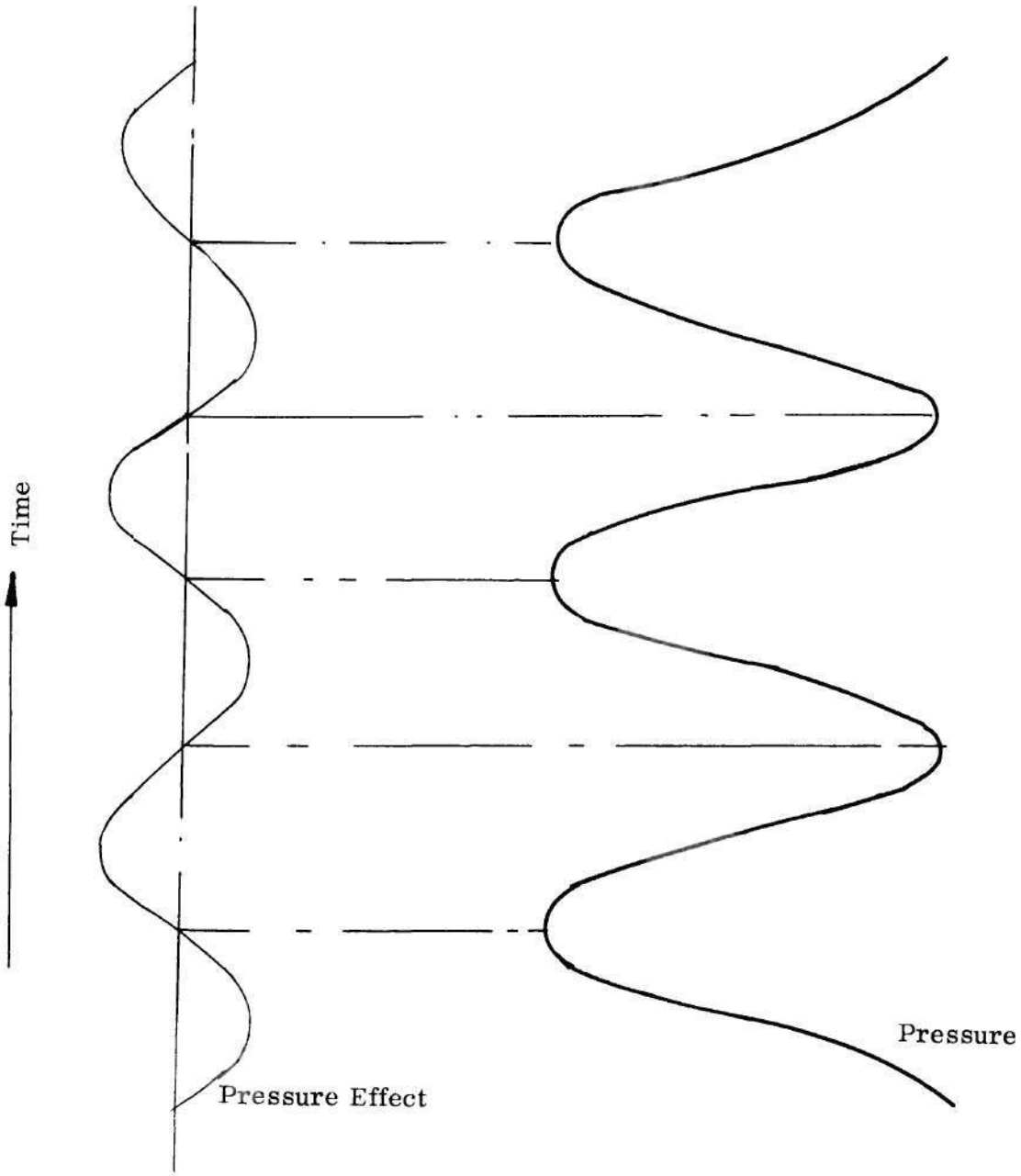

Figure 15. Pressure Effect Measured as Differential of Pressure Change.

errors may arise from slight change in alignment of pressure vessel with punch pressure machine, non-uniformity of pressure distribution on specimen, presence of oil under punched or welded joints and bad thermal contact. The magnitude of random errors vary from specimen to specimen and depends on the size, shape of specimen and specimen holder, the manner of mounting the specimen in holder and the method of affixing the thermocouples to the specimen. To be able to check these influences, each specimen was furnished with two thermocouples. The deviations between these are within $\pm$ 3 per cent as recorded on the visicorder. The mechanical deformation of the specimen involved in attaching thermocouples and local structural change such as in grain size and oxidation caused by heat of resistance welding of thermocouple on the specimen may also contribute to these deviations. As a matter of record, the welded and punched thermocouples showed no difference in results for the same material. However, the surface condition was important. For example, thermocouples welded on rough polished round specimen surfaces gave consistent and repetitive results.

The random errors could have been minimized by performing the experiments at highest possible pressure in order to magnify temperature and pressure variations. Owing to the limitations in our pressure generating techniques, large pressures could not be achieved. The compression experiments were conducted with a frequency of 4 c.p.s. in order to approach an ideal adiabatic condition. This was necessary not only for the temperature stability during compression but also for an accurate measurement of temperature and pressure variations. Materials with lower thermal conductivity are expected to exhibit the greatest deviations from the ideal

adiabatic condition. This occurs because the heat exchange to the thermocouple takes place through the specimen surface and the thermal coupling to the bulk of the specimen is relatively poor.

The temperature and pressure variations were recorded simultaneously as continuous curves shown in Figure 16. The average value of the temperature and pressure variations were obtained graphically. For this purpose, the widths of the deflections were measured by drawing parallel lines across the peaks of five cycles on an average. The accuracy of such measurements was influenced by the line thickness on the recording paper which was about 1 mm. Measurements were taken from the same side of the line to minimize the line thickness error. The different random errors from all possible sources do not exceed 6 per cent. When combined, the systematic and random errors are within a limit of 8 per cent.

Evaluation of Experimental Results

The baselines of temperature and pressure curves were set on the opposite edges of recording paper of the visicorder. Thus under cyclic compression the two deviations moved in opposite directions, thereby, the two curves can be easily separated (Figure 16). At the outset the temperature change is due partly to internal friction. The temperature equilibrium is obtained after the heat of internal friction is compensated by the heat losses build up in subsequent cycles. Conversion factors discussed in Appendices B and C were used to convert the graphical deflections of temperature and pressure variations into degrees centigrade and Kg/mm^2 respectively. Table 2 lists the total variations in temperature and

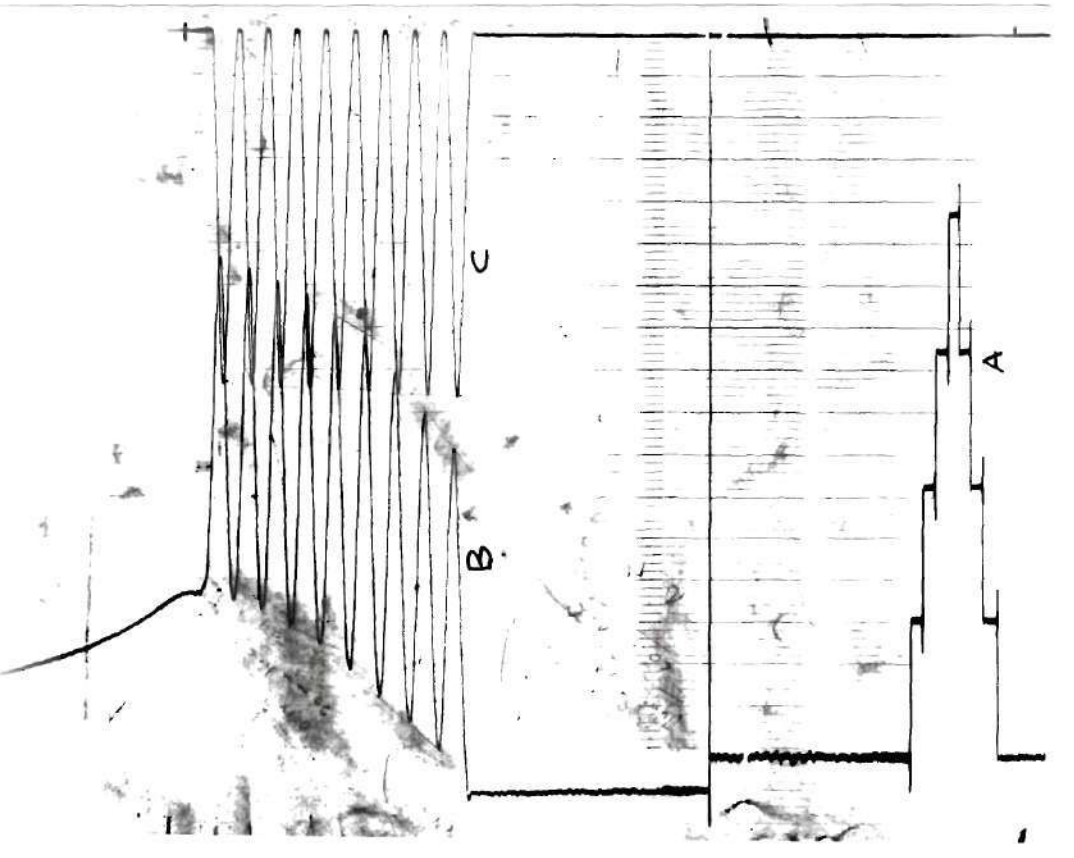

A. Temperature calibration curve

B. Temperature variation curve

C. Pressure variation curve

Figure 16. Typical Curves of Temperature Calibration and of Temperature and Pressure Variations.

pressure for each element under investigation. The ratio of the experimental values of temperature change to pressure change are also listed in Tables 2 and 3, and are plotted in Figures 17 through 20.

The equivalent heat of adiabatic compression per unit pressure can be calculated from the ratio of measured temperature change to pressure change for each element. The typical example of this calculation is given in Appendix D. The physical constants used for all the calculations in this paper are listed in Table 1. The internal energy change can be calculated by subtracting the mechanical work done on the specimen from the heat change. In the case of compression, however, the mechanical work done on the specimen was practically negligible. This was found by calculating the work done on the specimens of several metals in compression. Appendix E shows a typical calculation. In compression the work is small enough to be ignored and, therefore, the change in heat energy per unit pressure $(\frac{\Delta Q}{\Delta P})$ is considered to be equal to the change in internal energy per unit pressure $(\frac{\Delta E}{\Delta P})$. In Table 2, the measured $\frac{\Delta Q}{\Delta P}$ (or $\frac{\Delta E}{\Delta P}$) values are given for all the elements under study. These are also plotted in Figures 21 through 24. Figure 25 depicts the thermoelastic behavior of Cs in compression at different working temperatures. All these measured values and their plots are very useful for a comparative study of elements over the periodic chart.

Thermoelastic Effect

The experimental results of the thermoelastic effect can be compared with the values calculated from the thermoelastic equation. The thermoelastic effect is defined as the change in temperature of a body during an adiabatic elastic

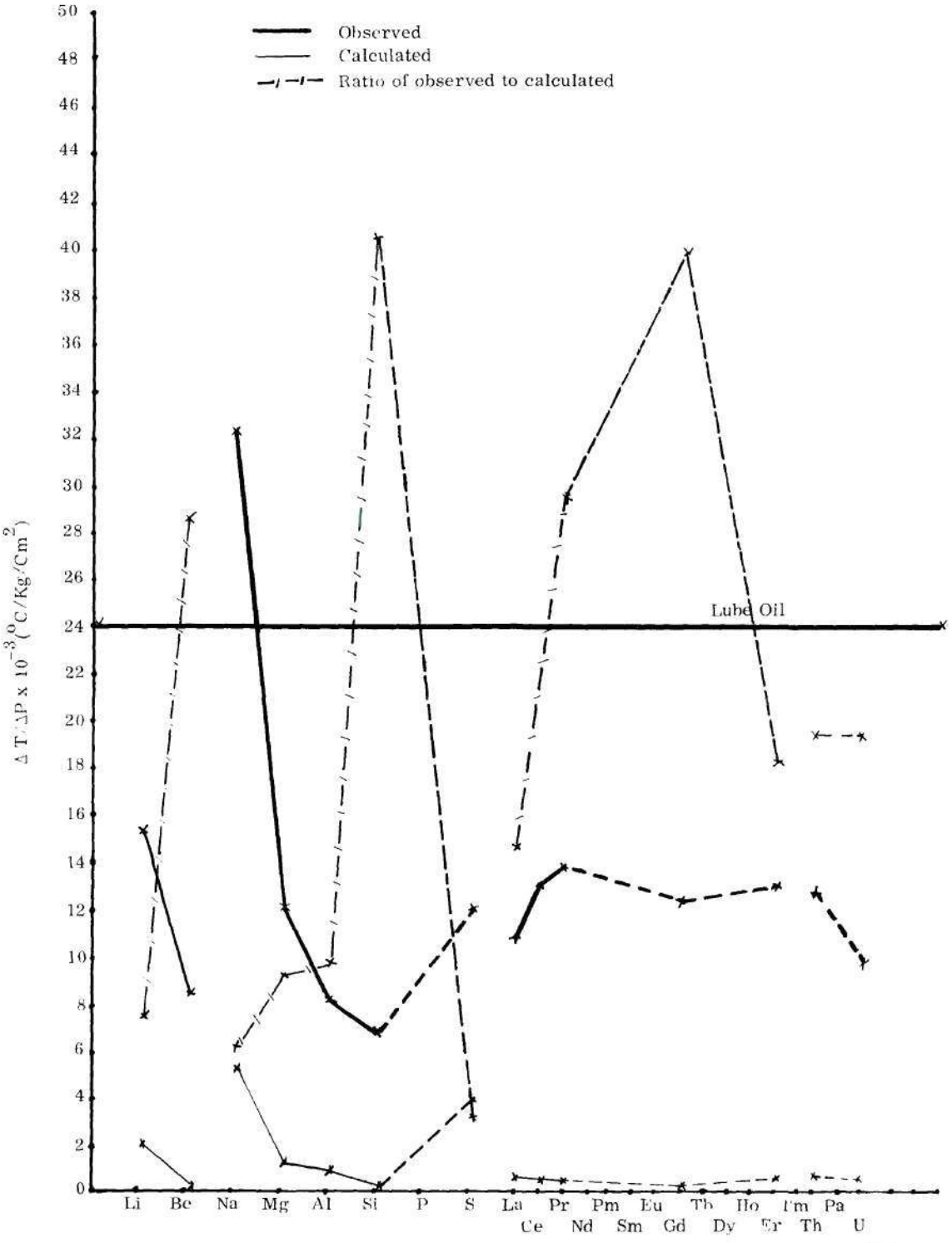

Figure 17. Comparison of the Observed and Calculated Values of $\frac{\Delta T}{\Delta P}$ in the Second, Third, Sixth-a and Seventh Period Elements.

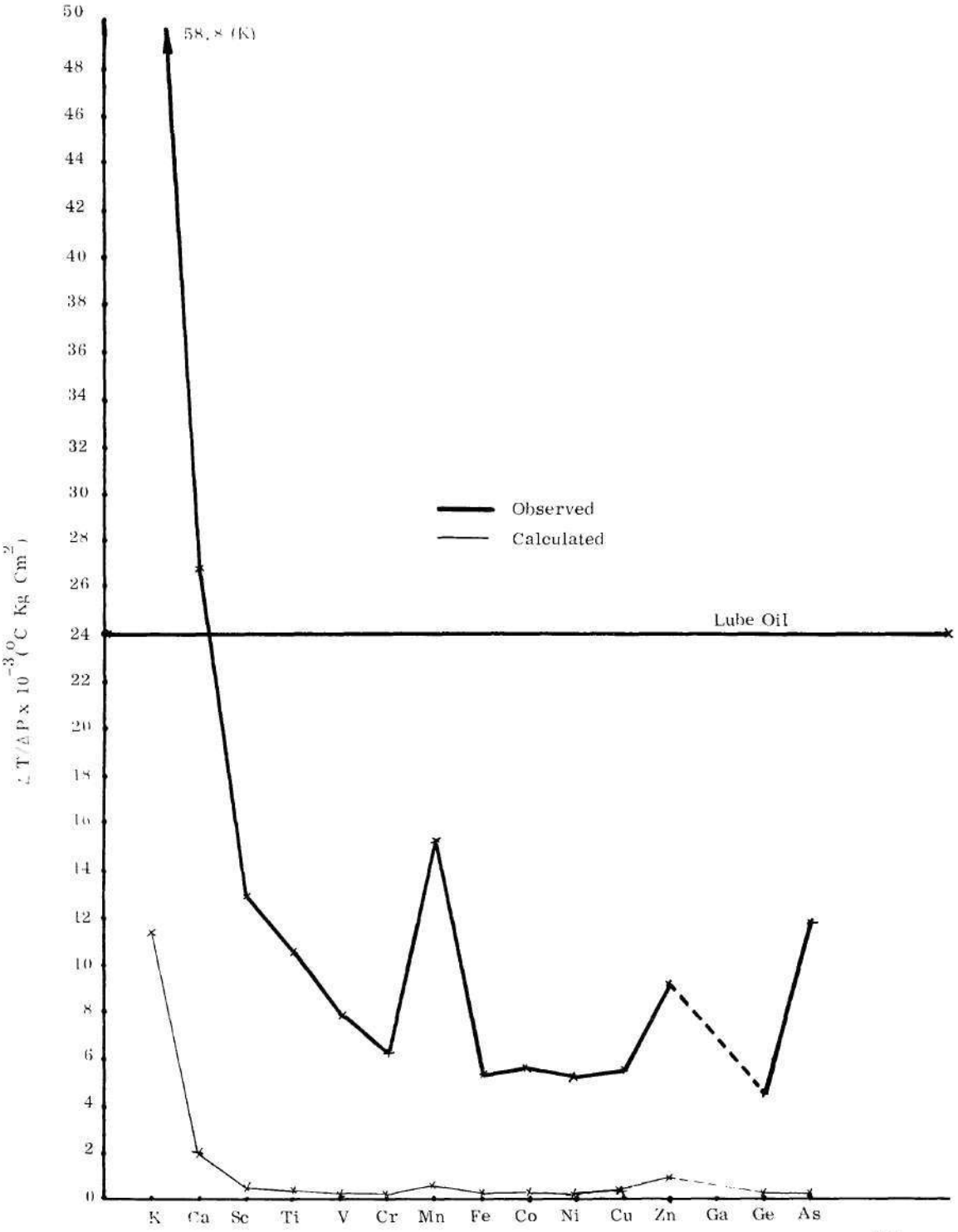

Figure 18. Comparison of the Observed and Calculated Values of $\frac{\Delta T}{\Delta P}$ in the Fourth Period Elements.

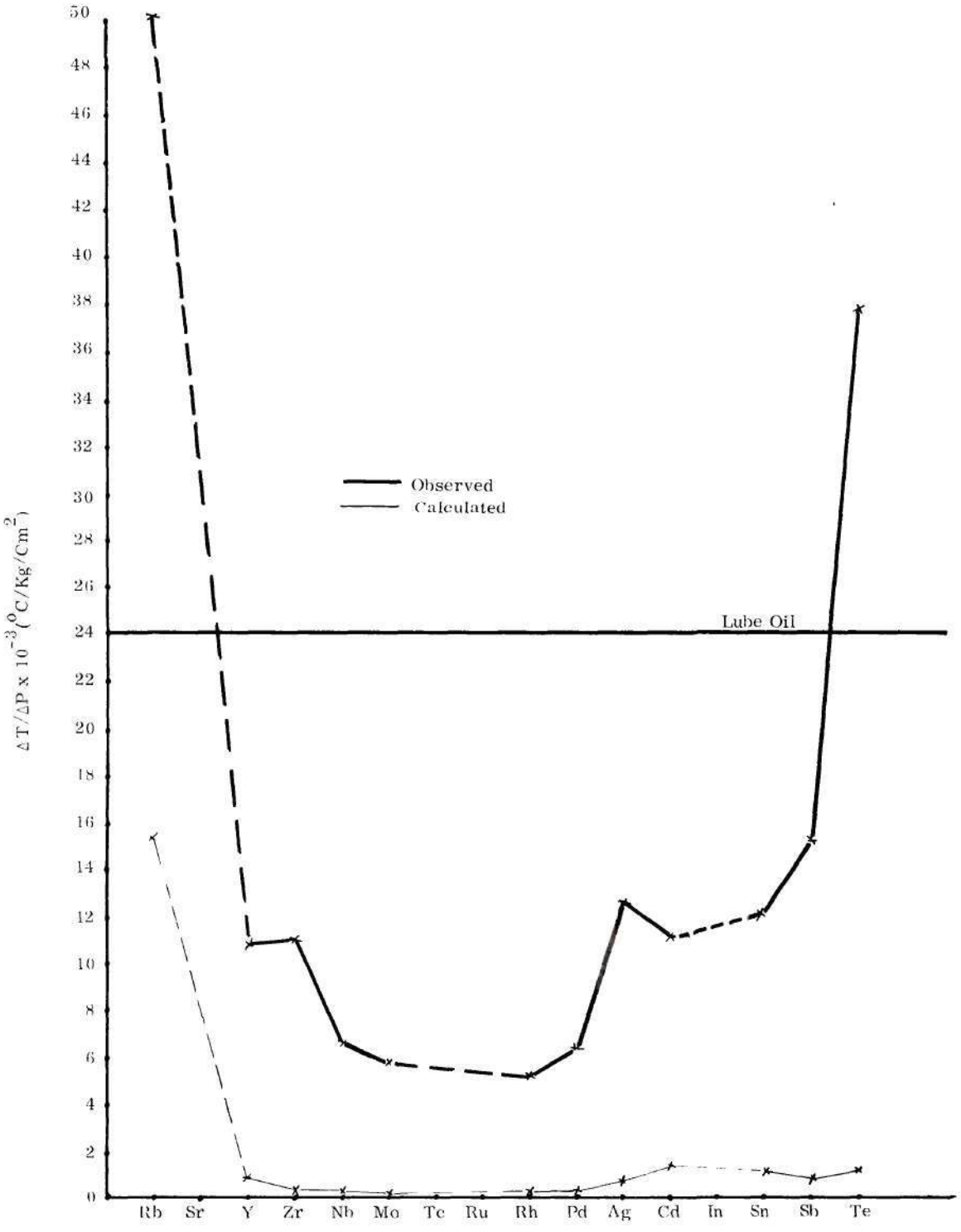

Figure 19. Comparison of the Observed and Calculated Values of $\frac{\Delta T}{\Delta P}$ in the Fifth Period Elements.

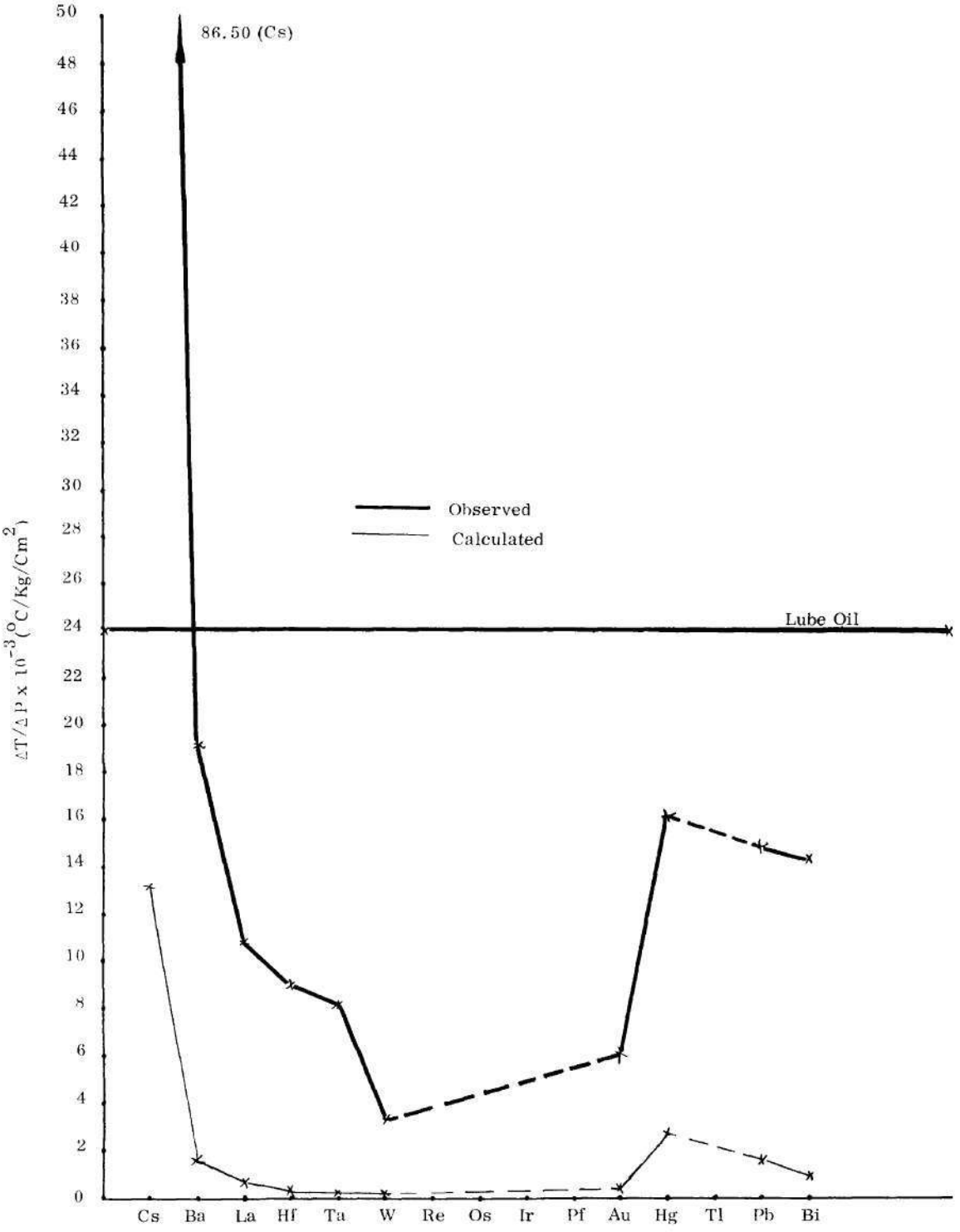

Figure 20. Comparison of the Observed and Calculated Values of $\frac{\Delta T}{\Delta P}$ in the Sixth Period Elements.

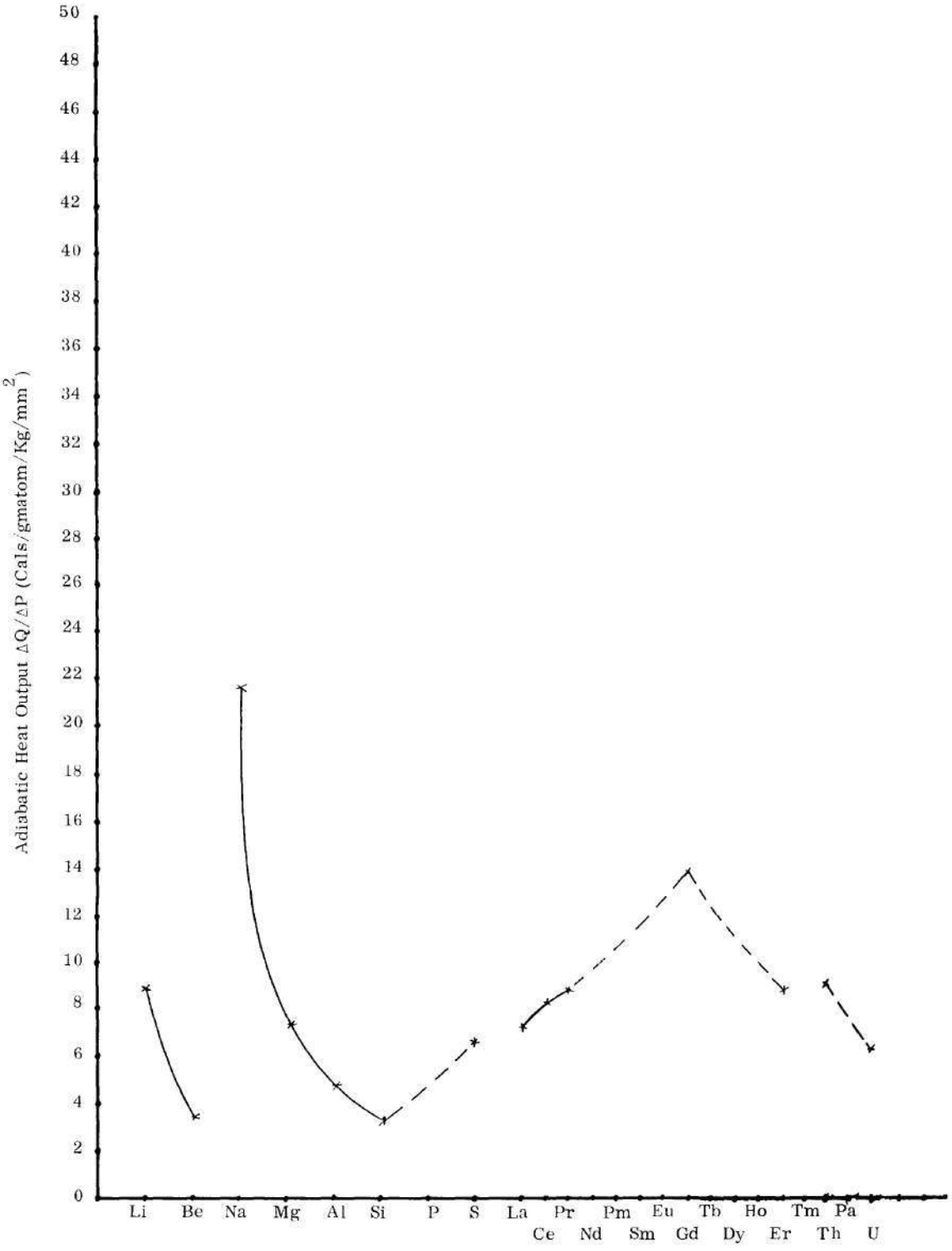

Figure 21. Thermoelastic Behavior of Elements in Compression over Second, Third, Sixth-a and Seventh Periods.

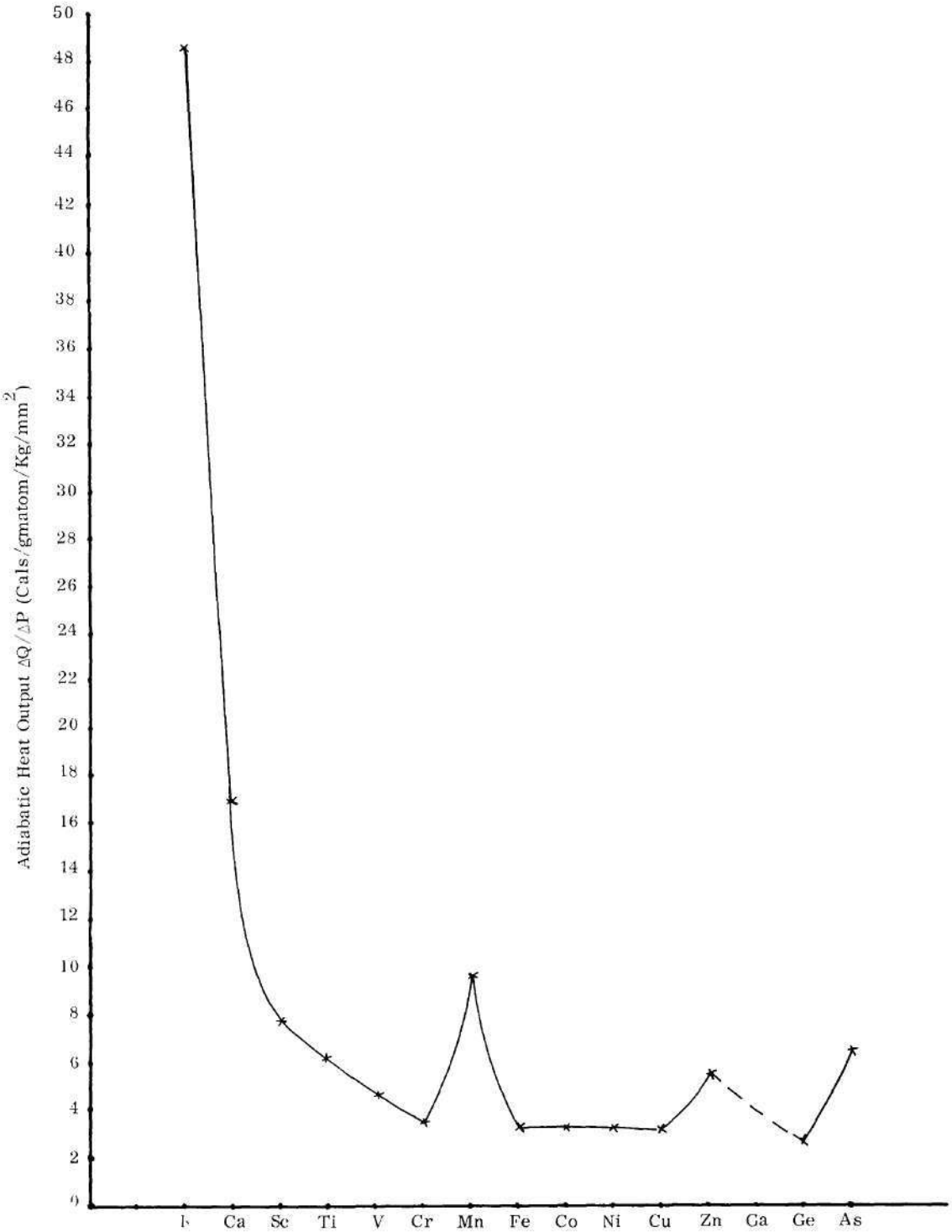

Figure 22. Thermoelastic Behavior of Elements in Compression over Fourth Period.

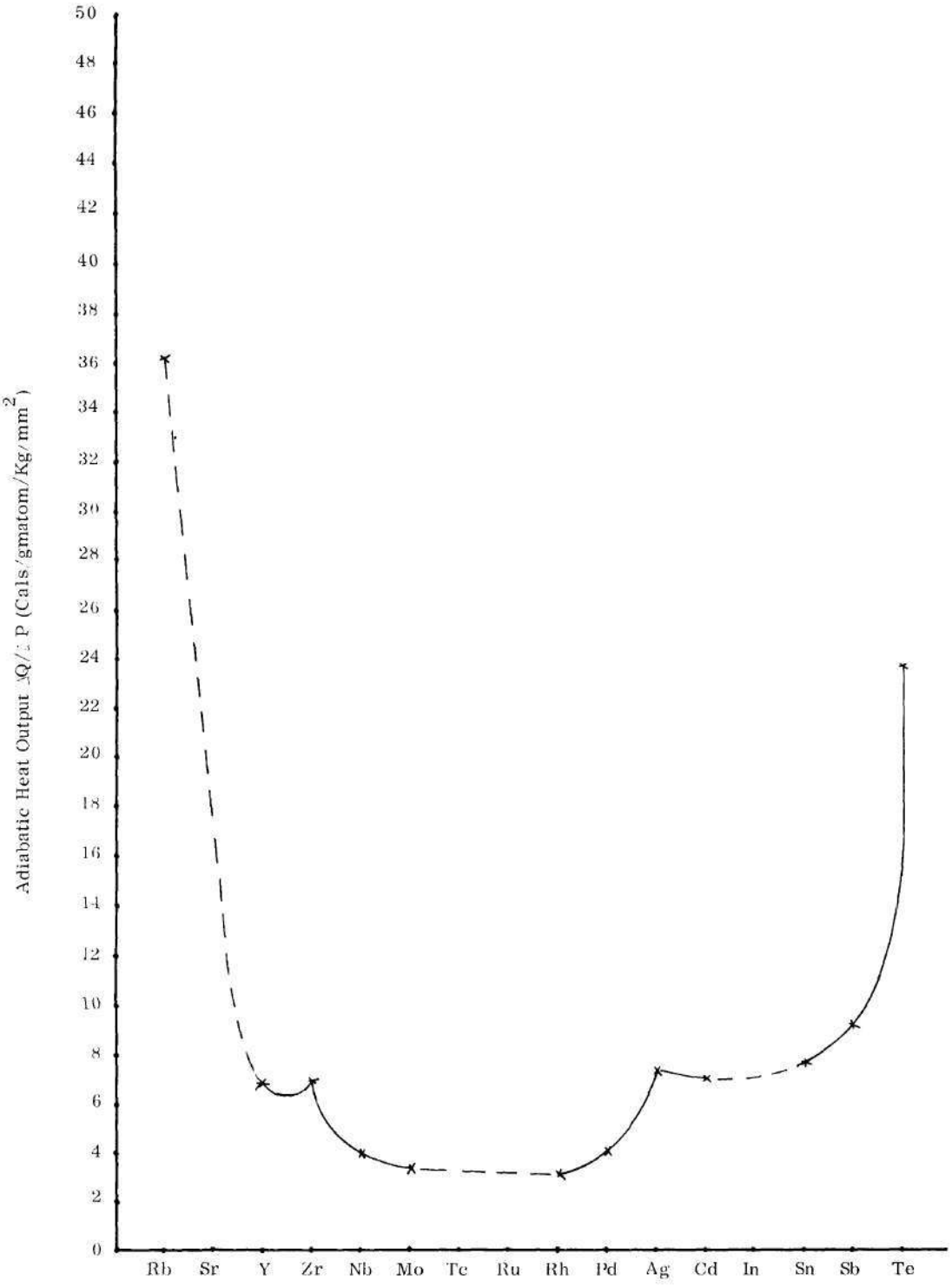

Figure 23. Thermoelastic Behavior of Elements in Compression over Fifth Period.

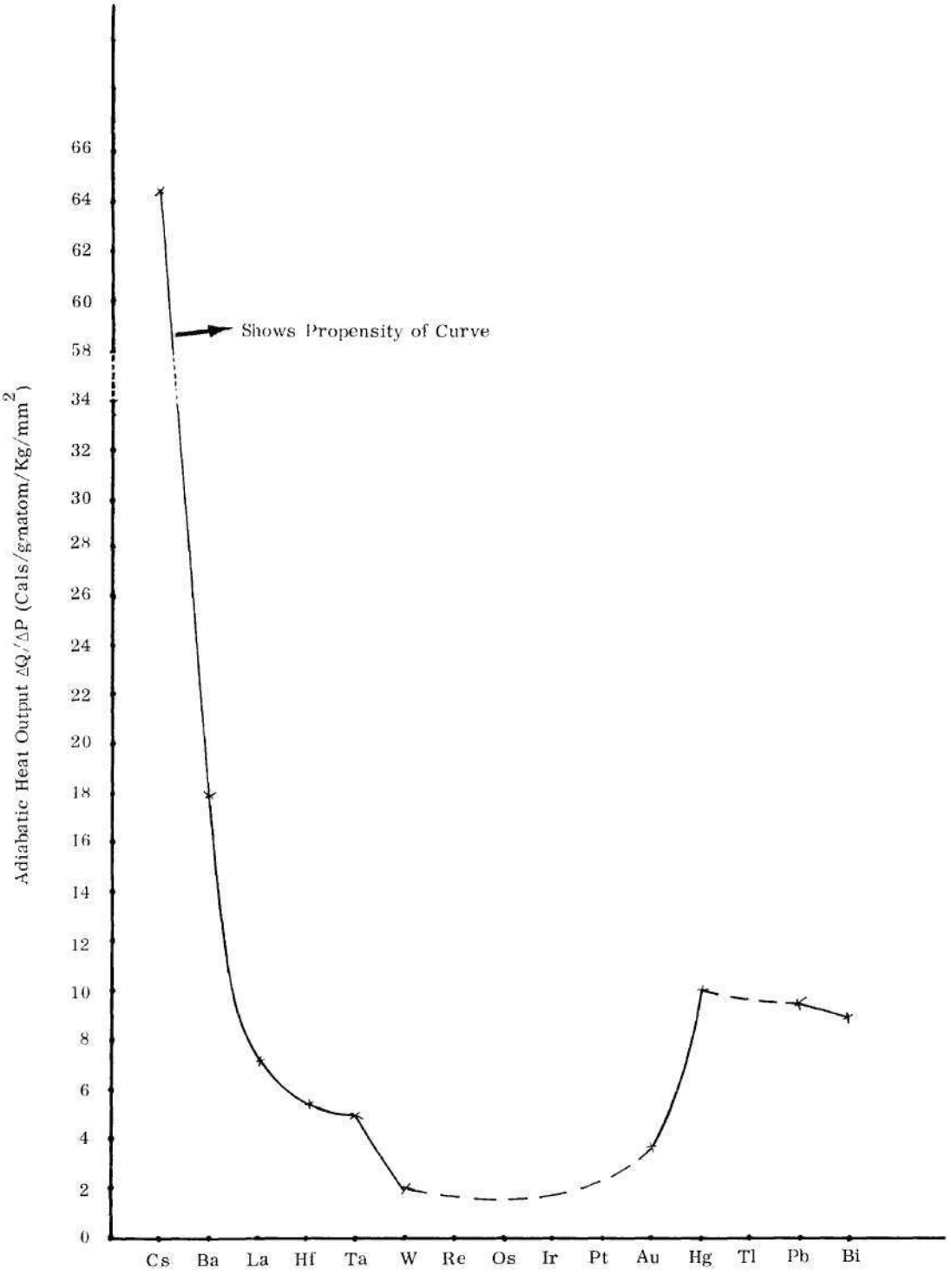

Figure 24. Thermoelastic Behavior of Elements in Compression over Sixth Period.

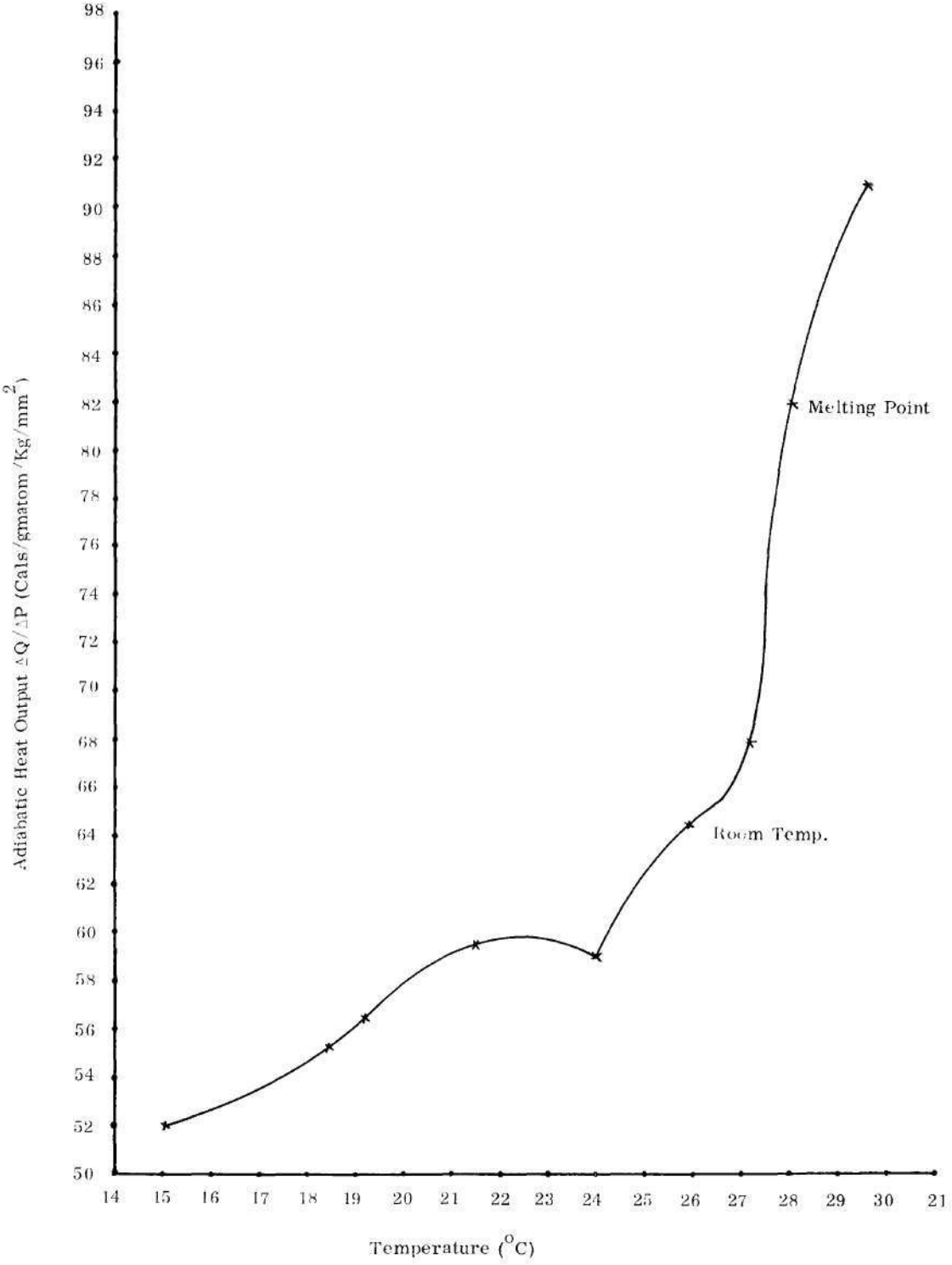

Figure 25. Thermoelastic Behavior of Cs in Compression at Different Working Temperatures.

deformation. At any temperature, the thermoelastic effect is an approximately linear function of the change in stress or pressure (In our investigations the experiments were carried out with small pressure changes). It is known that under adiabatic conditions, the temperature of a metal bar is decreased by an elastic elongation and is increased by an elastic compression (28). All metals which elongate on heating behave in this manner.

The thermoelastic effect should also be a nearly linear function of temperature, although increasing deviations from linearity must be expected as the temperature is raised, especially when approaching the melting point. It is noted, however, that the thermoelastic effect changes appreciably near the Curie temperature in case of ferromagnetic materials.

Lord Kelvin (29) derived an equation for the thermoelastic effect from the thermodynamic postulates. The following equation shows how a relationship between the temperature and stress changes for an elastic elongation can be established from the fundamental thermodynamics:

$$\frac{\Delta T}{\Delta \sigma} = - \frac{T \alpha V}{Cp}$$

where α is the coefficient of linear thermal expansion, V is the atomic volume, Cp is the specific heat and T is the temperature in ^{o}K. The sign of the temperature change ΔT is opposite to that stress change $\Delta \sigma$.

In case of an elastic compression, however, the thermoelastic equation takes a different shape as given below:

$$\frac{\Delta T}{\Delta P} = + \frac{T \beta V}{Cp} \quad ,$$

where β is the coefficient of cubical thermal expansion and ΔP is the change in pressure. It may also be noted that the sign of the temperature change is the same as that of the pressure change.

The ratio of the change of temperature to pressure ($\frac{\Delta T}{\Delta P}$) for each element under investigation was calculated applying the above equation. A calculation of $\frac{\Delta T}{\Delta P}$ from the thermoelastic equation is illustrated in Appendix F. The calculated values of $\frac{\Delta T}{\Delta P}$ are listed in Tables 2 and 3 and are also drawn along with the experimental values in Figures 17 through 20. The ratios of the observed to calculated values of $\frac{\Delta T}{\Delta P}$ are listed in Tables 2 and 3. A comparison of the experimentally observed values of $\frac{\Delta T}{\Delta P}$ with the calculated ones (Figures 17 through 20) shows that the observed values are much larger than the calculated values ranging somewhere between 3 to 55 times. It is remarkable that in case of alkali metals and sulfur the observed values are from 3 to 7.5 times the calculated values. The ratios of the observed to calculated values of $\frac{\Delta T}{\Delta P}$ were plotted in Figure 17 for second, third, sixth-a and seventh periods. The ratios between observed and calculated values are plotted in Figure 26 for the fourth, fifth and sixth periods for a comparison of the transition elements. It is interesting to note that Figure 26 shows a systematic pattern in distribution of this ratio over the three periods. The peaks in the ratio of 30 to 40 almost superimpose in the fourth column, the Ti column, whereas the minima superimpose at the low melting Zn column and then it goes up again. It is probable that the minimum is at the thirteenth column

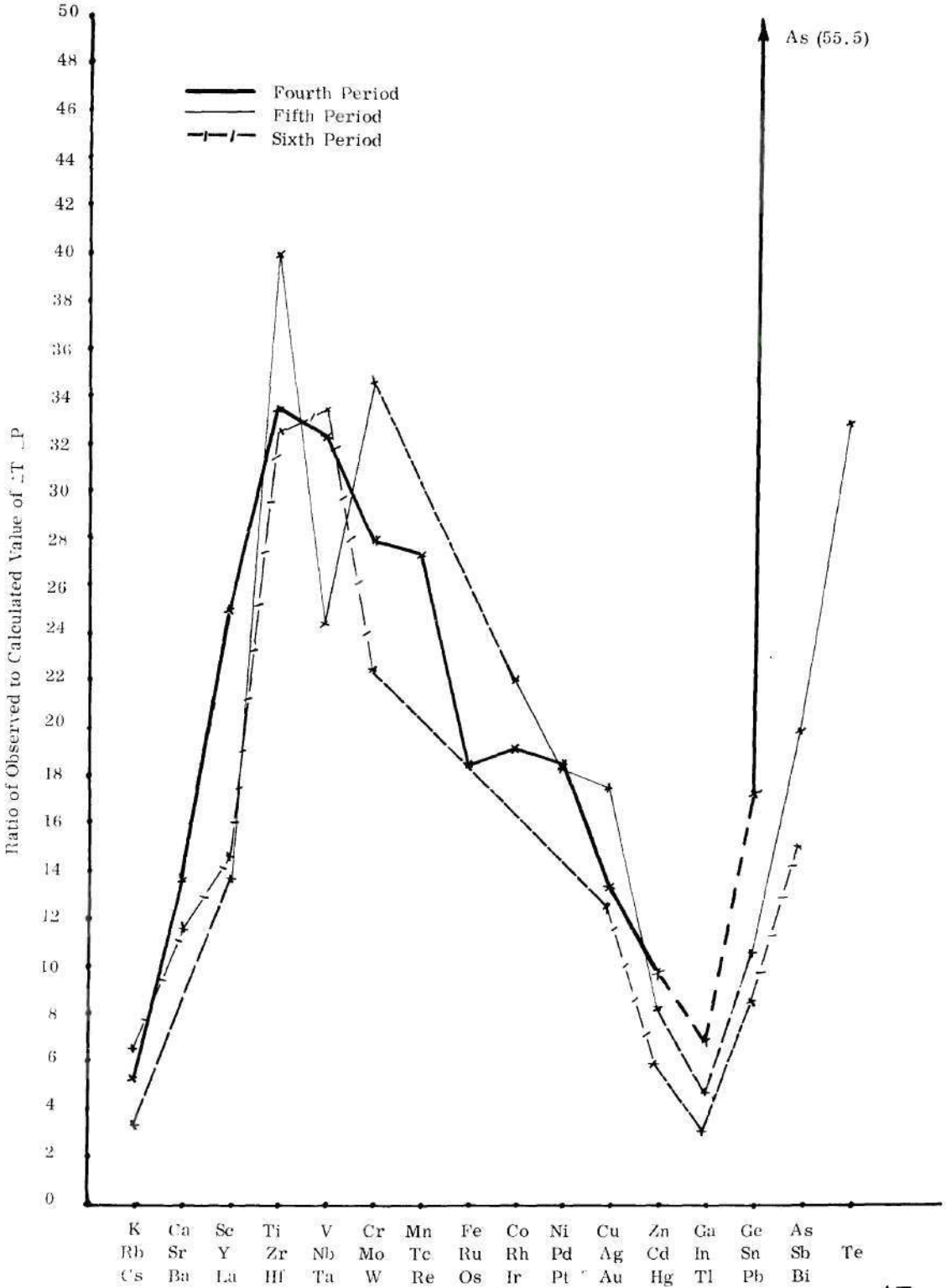

Figure 26. Distribution of the Ratio of Observed to Calculated Value of $\frac{\Delta T}{\Delta P}$ in Fourth, Fifth and Sixth Period Elements.

or the Ga column. Unfortunately no metals from this column were tested. Estimated values are nevertheless inserted in Figure 26. This trend suggests that a systematic basis for the understanding of bonding effects may be found in the thermoelastic results. On the same basis the bonding and electron transfer in metals in compression could be explained. However, it should be noted that the short periods behave differently with respect to the ratio of observed to calculated values of $\frac{\Delta T}{\Delta P}$ as represented by sulfur. Besides in the long periods, this ratio seems to increase with the period number. At this stage, it cannot be explained, since the elements in these columns are bonded partly by the Van der Waal's forces. Investigations in plastics and similar materials may be necessary before this behavior could be accounted for.

Heat can change the atomic distance of a metal and gives rise to electron movement between its outer and inner shells resulting in phase transformations. In a similar way stress or pressure should be expected to produce the same changes. When a metal is heated, the atoms vibrate at higher frequencies. The solid expands because the repulsive forces increase faster when atoms approach each other than the attractive forces increase when atoms are pulled apart. With reference to Figures 5 through 7 (Chapter II), d-bonding will be favored at the cost of outer (s+p) bonding when transition metal atoms approach each other, whereas outer-bonding becomes more favorable when the atomic distance is increased. Upon heating the average atomic distance increases but the instantaneous minimum atomic distance will be smaller and the instantaneous maximum distance will be larger. The effect of the minimum atomic distance will be overwhelming on the

electron distribution. This will lead to an increase of d-electron bonds in Ti with increase in temperature. This effect will be practically compensated by the influence from the time the atoms are at larger distances.

Uniaxial stress or triaxial stress (compression) produces a similar effect on the electronic distribution between outer and inner electrons. In uniaxial stress the atoms are drawn apart in the direction of the applied stress, but are brought together in the two directions perpendicular to the stress. Here again we see that the effects of atomic distance on the electron distribution are composed of two opposite and almost compensating influences.

In view of the similarity of effects of temperature and uniaxial stress, the thermoelastic effect can be calculated from thermal expansion with reasonable agreement (30). In case of a biaxial or triaxial stress (pressure), however, this may not be true. In compression for example, there are no compensating effects. This is because of the fact that with the increase in pressure the atoms from all directions only approach each other. This results in a change in the atomic distance in only one direction. The ultimate electronic changes in compression are, therefore, cumulative, and should be larger than in case of heating or stretching. This is the reason why the measured $\frac{\Delta T}{\Delta P}$ values in compression have been found to be greater than the corresponding values in stretching (30). Because of larger electronic changes in compression, the measured $\frac{\Delta T}{\Delta P}$ values should be larger than the $\frac{\Delta T}{\Delta P}$ values calculated from the thermoelastic equation. This agrees fairly well with our compression results (Tables 2 and 3). In general, the observed thermoelastic effects are larger than the effects calculated from the thermoelastic

equation. When we compare the alkaline metals (in which no electronic transfer between different shells can occur) with the transition metals, it becomes obvious that the alkali metals being more compressible and weakly bonded exhibit the highest thermoelastic effects ($\Delta Q/\Delta P$ values) as expected. W being the least compressible and most strongly bonded gives the least value of $\frac{\Delta Q}{\Delta P}$. However, the ratio between the observed and calculated values of $\frac{\Delta T}{\Delta P}$ vary in a regular manner over the periodic chart and in a manner agreeing with an additional thermoelastic effect due to electron movement in the transition metals.

In case of alkali metals, the observed $\frac{\Delta T}{\Delta P}$ values are only 3 to 7 times the calculated $\frac{\Delta T}{\Delta P}$ values. This makes it quite probable that no electronic changes have taken place in compression of these metals. The electronic part of heat of compression is dependent on the product of promotion energy and number of electrons moved between the outer and inner shells. The heat of compression for the alkali metals is composed mainly of the atomic vibrational energy. The ratio of measured to calculated values of $\frac{\Delta T}{\Delta P}$ decreases from 7.5 at Li over 6.1 at Na, down to 5.2 for K and 3.2 for Rb and jumps to 6.5 for Cs. This agrees with the fact that there are probably no electron movement in the first four alkali metals (no phase changes with increasing pressure), but a slow drop of electrons to inner shells in Cs (phase change with pressure).

Several transition metals exhibit thermal phase changes expressing electronic redistribution. It is known that in diffusion, the activation energy ΔQ is temperature dependent in Ti column elements (31). It seems quite reasonable to believe that in the Ti column elements the temperature has a pronounced

influence on the movement of electrons between outer and inner shells. This is also consistent with our experimental results that for the Ti column elements the observed heat of compression $(\frac{\Delta Q}{\Delta P})$ is many times greater than the corresponding calculated values. As mentioned before, Figure 26 also shows that the peaks superimpose at the Ti column.

Since pressure changes the interatomic distance of a metal, which in turn causes electron movement from the outer to the inner shells; hence the internal energy change per unit pressure can be related to the promotion energy which in fact is a part of internal energy change. In other words, such electronic movements due to promotion energy is measurable as a part of the internal energy change. According to the Engel concept, the bonding electrons maintain their specific character in the solid state as well as in free atoms. The spectroscopic data for the free atom, therefore, could be used in this analysis. On the basis of the spectroscopic data, Brewer (20) calculated the promotion energy for the electronic configurations $d^{n-1}s$ and $d^{n-2}sp$ for the transition elements in fourth, fifth and sixth period. These are listed in Tables 4 and 5. Using the spectroscopic data, Brewer (20) also plotted the relative promotion energy between $d^{n-1}s$ and $d^{n-2}sp$ electronic configurations for the transition elements in the fourth, fifth and sixth periods, which are presented in Figures 27 through 29 respectively.

As for each electronic configuration, there are several spectroscopic states corresponding to different combinations of spin and orbital momenta of the electron, the promotion energy of each configuration is shown as a band in Figures 27, 28 and 29. With increasing nuclear charge from left to right in a transition element

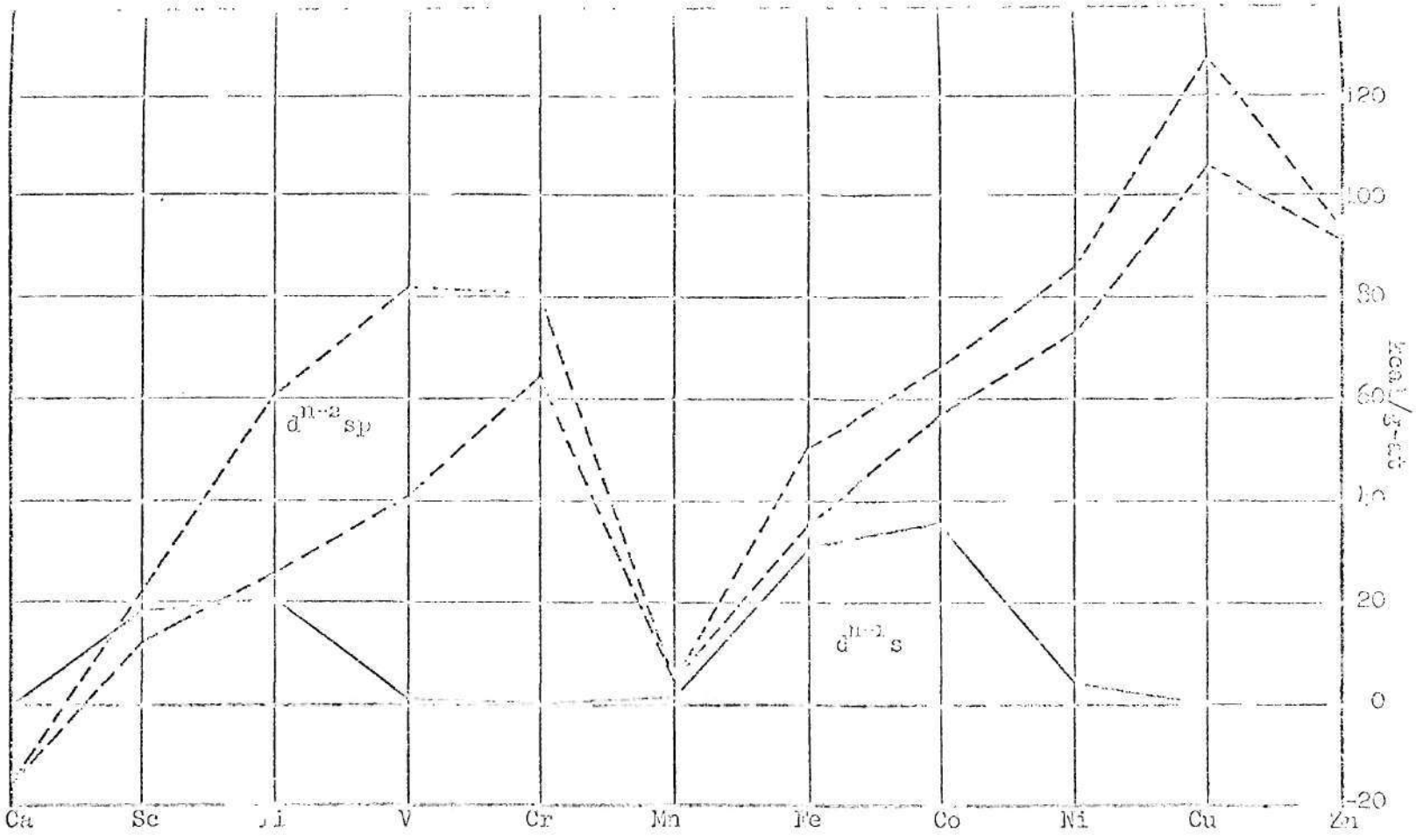

Figure 27. Relative Promotion Energy of $d^{n-1}s$ and $d^{n-2}sp$ Electronic Configurations for the Fourth Period Elements.

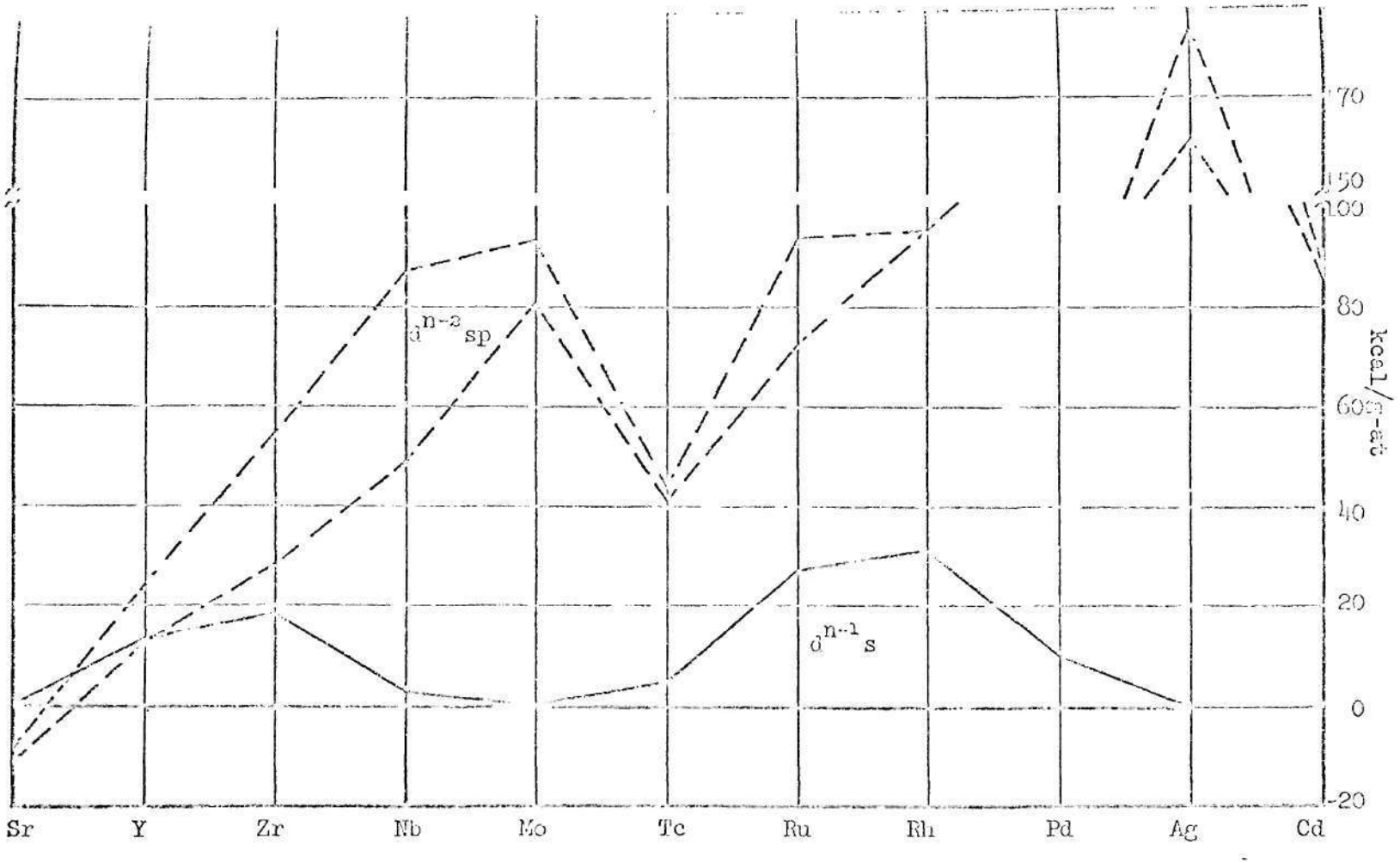

Figure 28. Relative Promotion Energy of $d^{n-1}s$ and $d^{n-2}sp$ Electronic Configurations for the Fifth Period Elements.

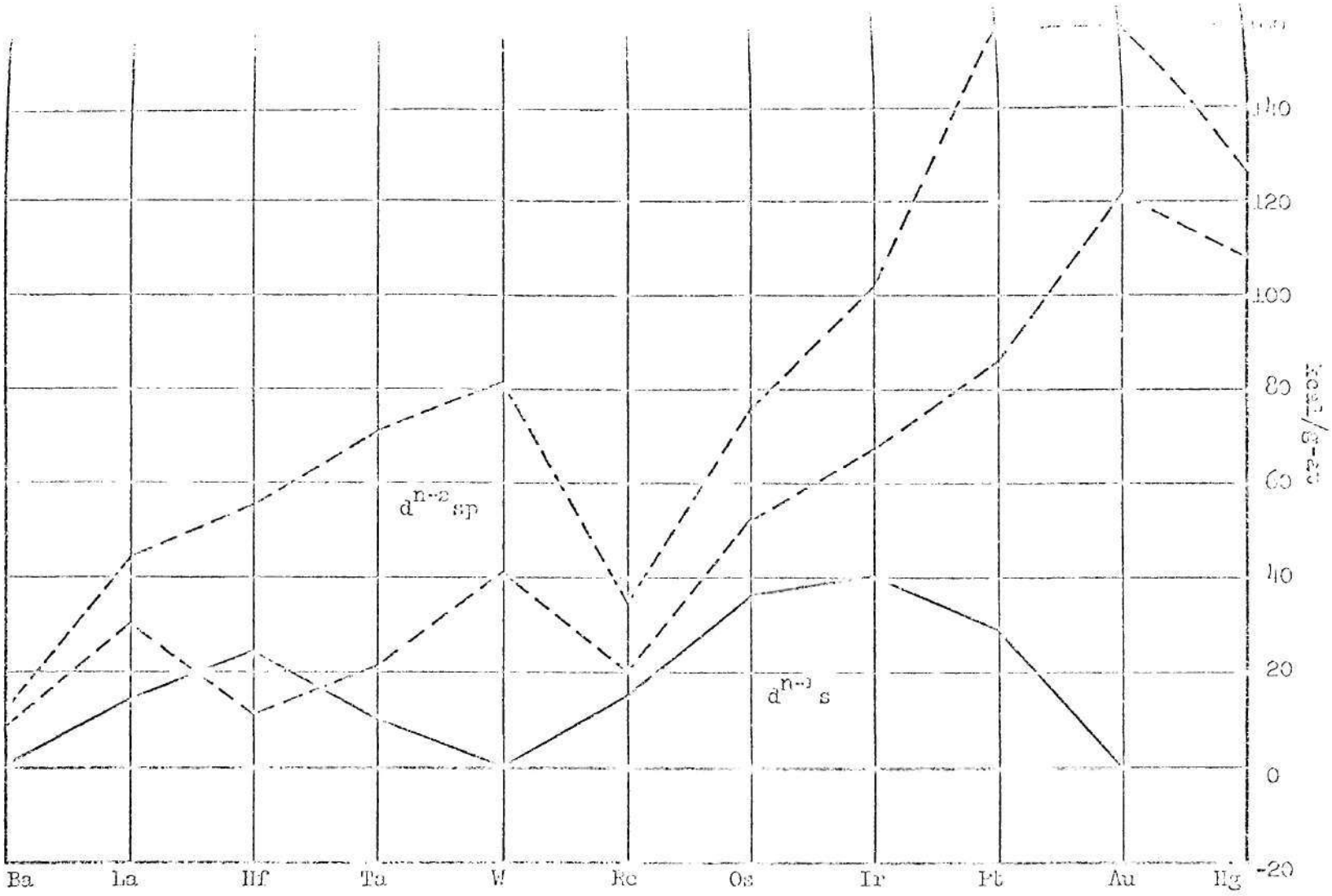

Figure 29. Relative Promotion Energy of $d^{n-1}s$ and $d^{n-2}sp$ Electronic Configurations for the Sixth Period Elements.

period, the d orbitals of the inner shell tend to get stabilized with regard to s and p orbitals of the outer shell. For the first three transition metals Ca, Sc and Ti of fourth period (Figure 27), we find that the two electronic configurations are rather close in respect of promotion energy. Also the B.C.C. ($d^{n-1}s$) and H.C.P. ($d^{n-2}sp$) structures should be expected to be close to each other in promotion energy. Thus, there would be a greater possibility of electron movement between the outer and inner shells under external pressure. For the metals V and Cr in the same period (Figure 27) the two configurations are quite apart since $d^{n-2}sp$ is a highly promoted electronic configuration in comparison to $d^{n-1}s$. Hence H.C.P. ($d^{n-2}sp$) structure will be unfavored with regard to B.C.C. ($d^{n-1}s$) structure. This leads us to expect that in this case there would be a small chance of electron transfer between the outer and inner shells under pressure. The promotion energies change in a similar manner in the corresponding column elements in fifth and sixth periods (Figures 28 and 29) leading to similar conclusions. The previous arguments are consistent with our original assumptions that both s+p and d electrons control the atomic size of transition elements, and that compression should give rise to the electron transfer between the outer and inner shells. However, electron movement should not be expected in non-transition metals, where either d shells do not exist or are saturated. In the event of any electron transfer to higher energy states, the promotion energy required would be extremely high.

CHAPTER V

CONCLUSIONS AND RECOMMENDATIONS

The results of the experimental investigations of the thermoelastic effect give more insight into the electronic behavior of elements. The following conclusions may be drawn on the basis of our investigations:

1. Because of the cumulative nature of the electronic changes in compression, the observed values of change in temperature per unit pressure are much larger than the calculated values (from the thermoclastic equation) ranging from 3 to 55 times.
2. One of the most interesting results is that the ratios of the observed to calculated values of change in temperature per unit pressure show a similar systematic pattern in its distribution over the fourth, fifth and sixth periods. In the transition metals the peaks almost superimpose at the Ti column, and fall toward minima superimposed at the low melting Zn or Ga column. The normal elements exhibit a minimum at the Zn or Ga column, thereafter a rapid increase takes place. The short periods behave differently as represented by sulfur. This indicates that the ratio of observed to calculated values of change in temperature per unit pressure has a distinct and definite bearing with electronic structure, bonding, and therefore electronic movements in metals during compression.

3. The ratio of observed and calculated values of change in temperature per unit pressure varies from 3 to 7 in the case of alkaline metals indicating either little or no electronic changes in compression of these metals. Most of their heats of compression are comprised of the atomic vibrational energy. This ratio decreases from 7.5 for Li to 6.1 for Na, further down to 5.2 for K and 3.2 for Rb and it increases to 6.5 for Cs. This is in agreement with the fact that there are probably no electron movement in the first four alkali metals (no phase changes with increasing pressure) but a slow transfer of electrons to the inner shells in Cs (phase changes with pressure).
4. The measured changes in temperature per unit pressure for the Ti column elements are higher than the corresponding calculated values (from the thermoelastic equation). Actually the ratios between observed and calculated values are highest in this column elements indicating the greatest electronic contribution. This is also interrelated with the fact that the activation energy, ΔQ, for diffusion is dependent on temperature, so far as Ti column elements are concerned.
5. In compression, the amount of mechanical work done to the specimens has been found to be negligible in comparison to the measured change of heat. In view of this, the equivalent heat energy change calculated from the measured change in temperature becomes practically equal to the change in internal energy.
6. With the exception of Mn, the change in heat or internal energy (per gram atom and unit pressure) is highest for the normal elements. It decreases to a minimum towards the middle of the period covering the transition elements.

In particular, Cs has the largest, whereas W has the smallest internal energy change with pressure. The heat or internal energy change is higher for the fourth column elements than for the sixth column elements. In general, the greater the compressibility and weaker the bond, the greater the thermoelastic effect becomes.

7. The electronic changes in elements in compression are cumulative and as such become larger than in stressing. This agrees with that the measured changes in temperature per unit pressure are greater than the corresponding values in stressing. This shows that in compression of a material the thermoelastic effect is more pronounced than in stressing.

8. The thermoelastic behavior of Cs in compression shows that the heat of compression (per gram atom and unit pressure) increases with temperature except near the melting range where some stagnation is noticed. The increase in liquid state is much more rapid than in solid state.

9. While selecting a suitable material for the specimen holder, some compression experiments on Teflon and Plexiglas showed that the heat of compression exhibited by Plexiglas is about half that of Teflon. Also Teflon showed a pronounced thermal after-effect indicating atomic or molecular rearrangement due to pressure changes.

10. The calculation for energy absorbed by the electron gas in compression of Na (Appendix A) indicates a clear disagreement of the electron gas theory with the observed facts.

It appears desirable to recommend the following for further investigations

in this area:

1. Work should be extended to complete the periodic chart elements with a particular emphasis on the low melting metals like Ga, In and Tl and also P, Se and Sr.
2. Investigations should include alloy systems, solid solutions, intermetallic phases, metastable phases like martensite, and metallic liquids which may reveal interesting information with respect to bonding and properties. Other interesting materials for investigation would be plastics, ceramics and organic compounds.
3. It would be of interest to observe the thermoelastic effect due to compression of materials at temperatures higher or lower than the room temperature especially a comparison at the Debye temperature of the elements.
4. A contrivance for the application of static pressure on the specimen should be designed. This will help make a comparative study of the thermoelastic effect with static and dynamic pressure devices.
5. Experiments ought to be carried out in biaxial stresses for comparison with uniaxial and triaxial effects.
6. It is recommended that work should be initiated to determine the quantitative role of atomic vibrational energy in internal energy change during stressing and compression of metals.
7. The reason for the systematic differences between the observed and calculated values of change in temperature per unit pressure should be further investigated.

APPENDICES

APPENDIX A

ENERGY ABSORBED BY ELECTRON GAS IN COMPRESSING Na

The ionization potential of Na = 5.12 eV.

(This is the energy required to pull the electron out of the potential of free atom.)

Since 1 eV/atom = 23.05 Kcals/gmatom,

the ionization potential of Na = 5.12 x 23.05

= 118.01 Kcals/gmatom.

Now, the bonding energy or heat of atomization = 25.90 Kcals/gmatom

(This is the energy required to separate the atoms from their lattice positions to free state.)

Hence, the total energy required = 118.01 + 25.90

= 143.91 Kcals/gmatom

Or E_1 = 144.00 Kcals/gmatom.

E_1 is the energy used to transform a Na lattice into Na ions and electrons. According to electron gas theory, this energy must be equivalent to the energy liberated when atoms form Na metal lattice with electron gas. When the negatively charged electrons are trapped in the positively charged field, the half of the potential energy is converted into radiations, and the other half is stored as the kinetic energy of electrons. Because of repulsion between positively charged ions and negatively charged electrons, the electrostatic potential must be larger

than 144.00 Kcals/gmatom, and the kinetic energy of electrons must, therefore, be larger than this quantity.

According to the electron gas theory, the energy absorbed in compressing Na can be calculated in the following manner:

The volume of 1 cm^3 of Na at 10,000Kg/cm^2 at room temperature = 0.888 cm^3.

That is, ΔV or change of volume or bulk compressibility

$$= 1-0.888 = 0.112 \text{ cm}^3.$$

Or the compression = 11.2%

The energy absorption in compression of Na,

E_2(per cm^3) $= 1/2.P.\Delta V$,

where P $= 10,000 kg/cm^2$, and $\Delta V = 0.112 \text{ cm}^3$

$$E_2 = 1/2 \times 10,000 \times 0.112$$

$$= 560 \text{ Kg cm}$$

$$= \frac{560}{100} \times 9.81 \text{ Joules}$$

$$= \frac{560 \times 9.81}{100 \times 4.19} \text{ cals/cm}^3$$

$$= \frac{560 \times 9.81 \times 23.67}{100 \times 4.19} \text{ cals/gmatom,}$$

where atomic volume of Na = 23.67 cm^3/gmatom

$$\text{or } E_2 = 312.00 \text{ cals/gmatom}$$

$$= 0.312 \text{ Kcals/gmatom}$$

Again, in case of 11.2 per cent compression, one side of 1 cm^3

$$= 3\sqrt{0.888} = 0.96 \text{ cm}$$

This means that the electrons are speeded up by 1/0.96 or about 4 per cent by compression. Thereby the kinetic energy of the electrons is increased by about 8 per cent, because $E_{Kin} = 1/2\ mv^2$.

Since the kinetic energy of the electron gas = 144 Kcals/gmatom, the increase in kinetic energy of electron gas = $\frac{8 \times 144}{100}$ = 11.52 Kcals/gmatom.

From Table 4, the observed thermoelastic heat output due to compression = 21.7 cals/gmatom/Kg/mm^2. Or the thermoelastic heat output = 21.7x100 cals/gmatom = 2.17 Kcals/gmatom.

It should be noted that 11.52 Kcals/gmatom (increase in kinetic energy according to the electron gas theory) does not appear in the theory of pairing of electrons. With respect to the electron gas concept, we should expect a great energy of absorption (11.520+0.312 = 11.832 Kcals/gmatom) due to the acceleration of electrons in compression, which is really many times larger and opposite in sign as compared to the actually measured thermoelastic heat output (2.17 Kcals/gmatom).

APPENDIX B

CALCULATIONS OF TEMPERATURE CALIBRATION

As mentioned in Chapter III and illustrated in Figure 12, a precision potentiometer was used to measure the potential difference on the calibration system. And it was easy to calculate the known small voltage drop across the four standard 1 ohm resistors quite accurately. This small potential was applied on the amplifier input. The galvanometer M 40-350A of visicorder recorded the deflection corresponding to the known potential. Thus a conversion factor was derived by equating the visicorder deflection in centimeters and the potential in volts. Further a given thermal e.m.f. can be evaluated as centigrates of temperature. The calculation is shown below:

For the amplifier gain range of 0.1 mV;

The potential difference on the calibration system = 1.082 V;

The voltage drop across the four standard 1 ohm resistors $= \frac{1.082}{80,000} \times 4$

$= 5.41 \times 10^{-5}$ V.

The corresponding deflection to 5.41×10^{-5} V as recorded on visicorder was

12.65 cms;

That is, a conversion factor of visicorder deflection in cms to potential turns out as; 1 cm $= 4.27 \times 10^{-6}$ V.

In our case, Chromel-Alumel thermocouple wires were used. The thermocouple calibration tables of Omega Co gave the thermal e.m.f. variation as 0.40mV

between $20^{o}C$ and $30^{o}C$ (room temperature). As such the final conversion factor is given as:

Since from above, $40 \times 10^{-6}V$ equals to $1^{o}C$;

Therefore, $4.27 \times 10^{-6}V$ (or 1 cm deflection) equals to $\frac{4.27}{40} = 0.1068^{o}C$.

Or 1 cm of temperature deflection = $0.1068^{o}C$ (with the amplifier gain range of 0.1 mV.) The potential 1.082 V on the calibration system and the visicorder deflection 12.65 cms were found to be fairly constant throughout the experiment.

APPENDIX C

CALCULATIONS OF PRESSURE CALIBRATION

Galvanometer M 100-350 of visicorder was used for pressure measurement. In order to check the voltage sensitivity (0.432 mV/in as given in the visicorder manual) of this galvanometer, the 80 K ohm and 39 K ohm of the temperature calibration system (Figure 13) were temporarily replaced by 1960 ohm and 997 ohm precision resistors respectively. The potential over 1964 ohm (1960 ohm + 4 ohm) was found to be 1.0450 volts as measured directly by the potentiometer. By introducing some adjustments in circuit connections, it was possible to use the same four-step switch of temperature calibration system to record deflections on the visicorder by the galvanometer used to record pressure changes. The total stepwise deflection was 10.2 cms. The calculations were done in the following manner:

The potential difference across 1964 ohm = 1.0450 V

The four-step deflection of galvanometer = $\frac{10.2}{2.54} = 4.02''$

This deflection of 4.02" was caused by a potential of $\frac{1.0450 \text{ V} \times 4}{1964}$

$= 2.128$ mV

Now,

Since 4.02" of four-step deflection equals to 2.128 mV per 4 ohm

Hence, 1" of deflection $= \frac{2.128}{4.02}$ mV/in

$$= 0.529 \text{ mV/in}$$

The aforesaid is the accurate value of voltage sensitivity of galvanometer M 100-350. This was adopted in further calculations to obtain a conversion factor of visicorder deflection in centimeters to pressure in p.s.i.

The certified pressure cell calibration is 3 mV/V for full deflection at 20,000 p.s.i. The deflection is rather linear. Feeding exactly 5 V to the pressure cell the visicorder galvanometer M 100-350 used should yield a deflection of

$$\frac{0.529 \text{ mV/in} \times 20,000 \text{ p.s.i.}}{3 \text{ mV/V} \times 5\text{V} \times 2.54 \text{ cm/in}} = 277.7 \text{ p.s.i./cm}$$

$$= 278 \text{ p.s.i./cm}$$

That is, 1 cm of pressure deflection = 278 p.s.i.g.

APPENDIX D

A TYPICAL CALCULATION OF ADIABATIC HEAT OF COMPRESSION

The adiabatic heat of compression of Al is calculated as an example:

Given:

Specific heat, Cp	= 5.911 cals/gmatom/^{o}C
Deflection of total temperature variation	= 12.5 cms
Deflection of total pressure variation	= 8.4 cms
Conversion factor of deflection in cm to the temperature in ^{o}C	= 0.1068 ^{o}C/cm
Conversion factor of deflection in cm to the pressure in p.s.i.	= 278 p.s.i./cm

Calculation:

ΔT, total temperature variation

$$= 12.5 \times 0.1068$$

$$= 1.335\,^{o}C$$

Δ P, total pressure variation

$$= 8.4 \times 278 \text{ p.s.i.}$$

$$= \frac{8.4 \times 278}{14.2} \text{ Kg/cm}^2$$

$$= 1.644 \text{ Kg/mm}^2$$

$$\frac{\Delta T}{\Delta P} = \frac{\text{total temperature variation}}{\text{total pressure variation}}$$

$$= \frac{1.335}{1.644} = 0.812\,^{o}C/Kg/mm^{2}$$

Hence, the adiabatic heat of compression of Al per unit pressure is given as,

$$\frac{\Delta Q}{\Delta P} = \frac{\Delta T . Cp}{\Delta P} = 0.812 \times 5.911$$

$$= 4.80 \text{ cals/gmatom/Kg/mm}^{2}$$

APPENDIX E

A TYPICAL CALCULATION OF MECHANICAL WORK INPUT TO SPECIMEN

As an example, a calculation of mechanical work input to Nb specimen is given below:

Given for Nb:

P, total pressure applied = 170.3Kg/cm^2

B, bulk modulus = $17.67 \times 10^5 \text{Kg/cm}^2$

V, atomic volume = $10.8 \text{ cm}^3/\text{gmatom}$

Calculation:

The compressibility is defined as

$$\beta = \frac{1}{B} = \frac{\Delta V}{\Delta P} \cdot \frac{1}{V}$$

$$\text{or } \Delta V = \frac{\Delta P}{B} \cdot V$$

where β = compressibility of the material

B = Bulk modulus

ΔV = Change in volume

$\Delta P = P - P_0$,

(P is the total applied pressure and P_0 is the original pressure, that is 1 atmosphere.)

V = atomic volume

The change in volume of Nb due to compression,

$$\Delta V = \frac{\Delta P}{B} \cdot V$$

$$\text{or} \quad \Delta V = \frac{P}{B} \cdot V \text{ while } P \gg P_0$$

$$= \frac{170.3}{17.67 \times 10^5} \times 10.8 \text{ cm}^3/\text{gmatom}$$

$$= 9.61 \times 10.8 \times 10^{-5} \text{ cm}^3/\text{gmatom}$$

Mechanical work input to Nb specimen,

$$W = P. \Delta V$$

$$= 170.3 \times 9.61 \times 10.8 \times 10^{-5} \text{ Kgcm/gmatom}$$

$$= \frac{170.3 \times 9.61 \times 10.8 \times 9.81}{100} \times 10^{-5} \text{ Joules/gmatom}$$

$$= \frac{170.3 \times 9.61 \times 10.8 \times 9.81}{4.19} \times 10^{-7} \text{ cals/gmatom}$$

Therefore, work done on 1 gm atom of Nb per unit pressure,

$$\frac{W}{\Delta P} = \frac{170.3 \times 9.61 \times 10.8 \times 9.81}{4.19 \times 1.703} \times 10^{-7}$$

$$= 24.2 \times 10^{-4} \text{ cals/gmatom/Kg/mm}^2$$

Now we have the equation,

Heat output - Work input = Change in internal energy

Or for per unit pressure,

$$\frac{\Delta Q}{\Delta P} - \frac{W}{\Delta P} = \frac{\Delta E}{\Delta P}$$

From Table 2, we find the measured $\frac{\Delta Q}{\Delta P}$ (heat change per unit pressure) for Nb to be 3.912 cals/gmatom/Kg/mm^2.

Substituting the values of observed $\frac{\Delta Q}{\Delta P}$ and calculated $W/\Delta P$ for Nb in the above equation:

$$3.912 - 24.2 \times 10^{-4} = \frac{\Delta E}{\Delta P}$$

$$\text{Or} \quad \frac{\Delta E}{\Delta P} = 3.9120 - 0.0024$$

As such for Nb, the change in internal energy per unit pressure

$$= 3.9096 \text{ cals/gmatom/Kg/mm}^2$$

It is obvious from the foregoing that the value of $\frac{W}{\Delta P}$ is extremely low in comparison to the magnitude of $\frac{\Delta Q}{\Delta P}$. Similar calculations were done for Na and W giving similar results. We, therefore, can safely ignore the negligible amount of mechanical work done on the specimen. That is, for our purpose,

$$\frac{\Delta Q}{\Delta P} \text{ practically equals to } \frac{\Delta E}{\Delta P}.$$

APPENDIX F

A TYPICAL CALCULATION OF $\frac{\Delta T}{\Delta P}$ FROM THERMOELASTIC EQUATION

The calculation of the ratio of the change of temperature to pressure $(\frac{\Delta T}{\Delta P})$ from thermoelastic equation for Mg in compression is done in the following way:

The thermoelastic equation for elastic compression is given as:

$$\frac{\Delta T}{\Delta P} = + \frac{T \beta V}{Cp \times 42.7} \ ^{o}C/Kg/cm^2$$

Where

$\beta = 3\alpha$

α = Coefficient of linear thermal expansion

β = Coefficient of cubical thermal expansion

The factor 42.7 appears in the above equation which is explained below:

Considering the units of the thermoelastic equation:

$$\frac{^{o}C}{Kg/cm^2} = + \frac{^{o}C \times \frac{1}{^{o}C} \times cm^3/gmatom}{cal/gmatom/^{o}C}$$

$$\text{Or } Kg/cm^2 = cal/cm^3$$

$$= 4.18 \text{ Joules}/cm^3$$

$$= 4.18 \text{ Newton meter/cm}^3$$

$$= 418 \text{ Newtons/cm}^2$$

$$= \frac{418}{9.8} \text{ Kg/cm}^2$$

$$= 42.7 \text{ Kg/cm}^2$$

Given for Mg:

Room temperature $T = 273 + 25 = 298^{\circ}K$

$\beta = 81.5 \times 10^{-6}$ unit volume/unit volume/$^{\circ}C$

Atomic volume $V = 14.00 \text{ cm}^3/\text{gmatom}$

Specific heat $Cp = 6.031 \text{ cals/gmatom/}^{\circ}C$

Substituting these values in the thermoelastic equation,

$$\frac{\Delta T}{\Delta P} = \frac{298 \times 81.5 \times 10^{-6} \times 14}{6.031 \times 42.7}$$

$$= 1.32 \times 10^{-3} \, ^{\circ}C/Kg/cm^2$$

Table 1. Physical Constants Used

Element	Cp Specific Heat (cals/gmatom/^{o}C)	B Bulk Modulus ($\times 10^{5}$ Kg/cm^{2})	V Atomic Volume (cm^{3}/gmatom)	β Coefficient of Cubical Thermal Expansion ($\times 10^{-6}/^{o}$C)
Li	5.830	1.390	12.990	135.000
Be	4.056	12.800	4.893	34.500
Na	6.736	0.832	23.670	211.800
Mg	6.031	3.390	14.000	81.500
Al	5.911	7.460	9.996	70.800
Si	4.550	10.080	12.070	9.210
S	5.620	1.820	16.360	189.000
K	7.030	0.406	45.470	249.000
Ca	6.350	1.760	25.860	67.200
Sc	6.030	6.500	14.890	30.000
Ti	6.035	12.600	10.630	25.050
V	6.063	16.530	8.350	24.900
Cr	5.721	19.420	7.230	25.200
Mn	6.373	12.690	7.390	67.800
Fe	6.090	17.160	7.100	35.100
Co	6.010	18.700	6.660	37.200
Ni	6.340	18.700	6.590	38.100
Cu	5.859	14.000	7.090	49.500
Zn	6.145	6.170	9.170	89.100
Ge	6.400	7.874	13.640	17.250
As	5.550	4.018	13.090	12.840
Rb	7.250	0.430	55.870	264.300

Table 1 (Continued). Physical Constants Used

Element	Cp Specific Heat (cals/gmatom/^{o}C)	B Bulk Modulus ($\times 10^{5}$ Kg/cm^{2})	V Atomic Volume (cm^{3}/gmatom)	β Coefficient of Cubical Thermal Expansion ($\times 10^{-6}/^{o}$C)
Y	6.313	4.780	19.950	36.000
Zr	6.294	9.150	14.060	17.550
Nb	5.946	17.670	10.800	21.210
Mo	5.948	28.000	9.390	14.940
Rh	6.174	28.010	8.270	25.200
Pd	6.278	19.100	8.880	34.500
Ag	5.827	10.180	10.280	57.600
Cd	6.294	4.850	13.000	91.800
Sn	6.410	5.200	16.280	63.600
Sb	6.085	7.800	18.400	35.700
Te	6.300	2.347	20.460	50.310
Cs	7.450	0.370	69.840	201.000
Ba	9.340	0.980	39.000	56.400
La	6.670	2.850	22.440	31.200
Ce	6.300	2.125	20.690	25.500
Pr	6.350	3.117	20.820	20.400
Gd	11.170	4.000	19.910	24.840
Er	6.690	4.188	18.460	36.900
Hf	6.248	11.150	13.640	18.030
Ta	6.151	21.050	10.900	19.650
W	6.065	31.860	9.530	13.770
Au	6.143	17.460	10.200	42.300
Hg	6.620	2.880	14.090	183.000

Table 1 (Concluded). Physical Constants Used

Element	Cp Specific Heat (cals/gmatom/^{o}C)	B Bulk Modulus ($\times 10^{5}$ Kg/cm^{2})	V Atomic Volume (cm^{3}/gmatom)	β Coefficient of Cubical Thermal Expansion ($\times 10^{-6}/^{o}$C)
Pb	6.420	4.220	18.270	87.000
Bi	6.225	3.600	21.300	40.230
Th	7.192	5.510	19.900	33.600
V	6.664	10.400	12.480	37.800

Table 2. Experimental Values

Element	1 Total ΔT (observed) ^{o}C	2 Total ΔP (observed) Kg/mm^2	3 $\frac{\Delta T}{\Delta P}$ (observed) $^{o}C/Kg/mm^2$	4 $\frac{\Delta T}{\Delta P}$ (calculated) from thermo-elastic eqn. $^{o}C/Kg/mm^2$	5 Ratio of 3 & 4	6 $\frac{\Delta E}{\Delta P}$ or $\frac{\Delta Q}{\Delta P}$ (observed) cals/gmaton/Kg/mm^2
Li	2.720	1.781	1.530	0.2050	7.5	8.900
Be	1.388	1.644	0.844	0.0295	28.5	3.423
Na	5.735	1.781	3.220	0.5230	6.15	21.690
Mg	2.051	1.703	1.204	0.1320	9.2	7.261
Al	1.335	1.644	0.812	0.0840	9.7	4.800
Si	1.170	1.723	0.680	0.0169	40.4	3.200
S	2.150	1.742	1.190	0.3850	3.1	6.700
K	10.470	1.781	5.880	1.1300	5.2	48.500
Ca	2.880	1.742	2.680	0.1930	13.5	17.010
Sc	2.240	1.742	1.290	0.0520	24.8	7.800
Ti	1.762	1.684	1.046	0.0312	33.5	6.313
V	1.335	1.723	0.775	0.0240	32.3	4.699
Cr	1.068	1.723	0.620	0.0223	27.8	3.547
Mn	2.691	1.762	1.527	0.0560	27.3	9.732

Table 2 (Continued). Experimental Values

Element	1 Total ΔT (observed) ^{o}C	2 Total ΔP (observed) Kg/mm^2	3 $\frac{\Delta T}{\Delta P}$ (observed) $^{o}C/Kg/mm^2$	4 $\frac{\Delta T}{\Delta P}$ (calculated) from thermo-elastic eqn. $^{o}C/Kg/mm^2$	5 Ratio of 3 & 4	6 $\frac{\Delta E}{\Delta P}$ or $\frac{\Delta Q}{\Delta P}$ (observed) cals/gmatom/Kg/mm^2
Fe	0.865	1.625	0.532	0.0290	18.4	3.240
Co	0.961	1.703	0.564	0.0290	19.1	3.390
Ni	0.886	1.703	0.520	0.0280	18.6	3.297
Cu	0.918	1.684	0.545	0.0405	13.4	3.193
Zn	1.495	1.644	0.909	0.0933	9.75	5.586
Ge	0.750	1.664	0.450	0.0260	17.3	2.880
As	2.150	1.742	1.190	0.0213	55.5	6.600
Rb	8.760	1.742	5.000	1.5300	3.25	36.250
Y	1.752	1.625	1.078	0.0793	13.6	6.805
Zr	1.858	1.684	1.103	0.0275	40.0	6.942
Nb	1.121	1.703	0.658	0.0270	24.4	3.912
Mo	0.961	1.684	0.570	0.0165	34.5	3.390
Rh	0.865	1.684	0.514	0.0234	22.0	3.173
Pd	1.068	1.684	0.634	0.0345	18.4	3.980

Table 2 (Continued). Experimental Values

Element	1 Total ΔT (observed) ^{o}C	2 Total ΔP (observed) Kg/mm^2	3 $\frac{\Delta T}{\Delta P}$ (observed) $^{o}C/Kg/mm^2$	4 $\frac{\Delta T}{\Delta P}$ (calculated) from thermo-elastic eqn. $^{o}C/Kg/mm^2$	5 Ratio of 3 & 4	6 $\frac{\Delta E}{\Delta P}$ or $\frac{\Delta Q}{\Delta P}$ (observed) $cals/gmatom/Kg/mm^2$
Ag	2.099	1.684	1.250	0.0715	17.5	7.284
Cd	1.858	1.684	1.103	0.1330	8.3	6.942
Sn	2.051	1.703	1.204	0.1130	10.7	7.718
Sb	2.627	1.742	1.508	0.0760	19.9	9.176
Te	6.840	1.810	3.780	0.1150	33.0	23.800
Cs	15.100	1.742	8.650	1.3200	6.5	64.500
Ba	3.300	1.723	1.920	0.1660	11.5	18.000
La	1.860	1.732	1.080	0.0738	14.6	7.200
Ce	2.270	1.742	1.310	0.0590	22.2	8.300
Pr	2.400	1.742	1.380	0.0470	29.5	8.800
Gd	2.180	1.762	1.240	0.0313	39.9	13.850
Er	2.270	1.742	1.310	0.0714	18.3	8.750
Hf	1.549	1.723	0.899	0.0276	32.5	5.617
Ta	1.388	1.693	0.820	0.0245	33.5	5.044

Table 2 (Concluded). Experimental Values

Element	1 Total ΔT (observed) ^{o}C	2 Total ΔP (observed) Kg/mm^2	3 $\frac{\Delta T}{\Delta P}$ (observed) $^{o}C/Kg/mm^2$	4 $\frac{\Delta T}{\Delta P}$ (calculated) from thermo-elastic eqn. $^{o}C/Kg/mm^2$	5 Ratio of 3 & 4	6 $\frac{\Delta E}{\Delta P}$ or $\frac{\Delta Q}{\Delta P}$ (observed) $cals/gmatom/Kg/mm^2$
W	0.587	1.723	0.340	0.0152	22.4	2.062
Au	1.025	1.684	0.609	0.0485	12.5	3.741
Hg	2.880	1.781	1.620	0.2730	5.9	10.140
Pb	2.435	1.625	1.500	0.1740	8.6	9.630
Bi	2.499	1.732	1.443	0.0960	15.1	8.983
Th	2.211	1.732	1.277	0.0658	19.4	9.184
V	1.698	1.742	0.975	0.0503	19.4	6.497

Table 3. Observed and Calculated Values of $\frac{\Delta T}{\Delta P}$

	0	1	2	3	4	5	6	7	8	9	10	11	12	13	14	15	16	17	18
1	n	H																H	He
2	He	Li 1.530 .2050 7.5	Be 0.844 .0295 28.5											B	C	N	O	F	Ne
3	Ne	Na 3.220 0.523 6.15	Mg 1.204 0.132 9.2	Al 0.812 0.084 9.7									Mg	Al	Si 0.680 .0169 40.4	P	S 1.190 0.385 3.1	Cl	Ar
4	Ar	K 5.880 1.13 5.2	Ca 2.680 0.193 13.5	Sc 1.290 0.052 24.8	Ti 1.046 .0312 33.5	V 0.775 0.024 32.3	Cr 0.620 .0223 27.8	Mn 1.527 0.056 27.3	Fe 0.532 0.029 18.4	Co 0.564 .0290 19.1	Ni 0.520 .0280 18.6	Cu 0.545 .0405 13.4	Zn 0.909 .0933 9.75	Ga	Ge 0.450 .0260 17.3	As 1.190 .0213 55.5	Se	Br	Kr
5	Kr	Rb 5.000 1.53 3.25	Sr	Y 1.078 .0793 13.6	Zr 1.103 .0275 40.0	Nb 0.658 0.027 24.4	Mo 0.570 .0165 34.5	Tc	Ru	Rh 0.514 .0234 22.0	Pd 0.634 .0345 18.4	Ag 1.250 .0715 17.5	Cd 1.103 .1330 8.3	In	Sn 1.204 .1130 10.7	Sb 1.508 .0760 19.9	Te 3.780 .1150 33.0	I	X
6	X	Cs 8.650 1.32 6.5	Ba 1.920 0.166 11.5	La 1.080 .0738 14.6	Hf 0.899 .0276 32.5	Ta 0.820 .0245 33.5	W 0.340 .0152 22.4	Re	Os	Ir	Pt	Au 0.609 .0485 12.5	Hg 1.620 0.273 5.9	Tl	Pb 1.500 0.174 8.6	Bi 1.443 0.096 15.1	Po	At	Rn
7	Rn	Fr	Ra	Ac	Th 1.277 .0658 19.4	Pa	U 0.975 .0503 19.4	Np	Pu	Am	Cm								

6a	Ce 1.310 .0590 22.2	Pr 1.380 .0470 29.5	Nd	Pm	Sm	Eu	Gd 1.240 .0313 39.9	Tb	Dy	Ho	Er 1.310 .0714 18.3	Tm	Yb	Lu

Note: The numerical entry below the symbol of an element gives values for the observed ($\Delta T/\Delta P$) in $^{o}C/Kg/mm^{2}$. The second entry is for the calculated ($\Delta T/\Delta P$) in $^{o}C/Kg/mm^{2}$ and the third entry is for the ratio of the observed to calculated values of $\Delta T/\Delta P$.

Table 4. Promotion Energies of $d^{n-2}sp$ Valence State (in kcal per mole)

Ground-state configurations										
s^2	ds^2	d^2s^2	d^3s^2 except*	d^5s except*	d^5s^2	d^6s^2 except*	d^7s^2 except*	d^8s^2 except*	$d^{10}s$	$d^{10}s^2$
Mg 63										
Ca 43	Sc 45-46, 53	Ti 45-54, 72-80	V 47-54, 81-88	Cr 71-80	Mn 53	Fe 55-70	Co 67-76	Ni(d^8s^2) 74-87	Cu 113-128	Zn 92-94
Sr 41-43	Y 43-49, 54	Zr 42-57, 66-74	Nb*(d^4s) 48-61, 74-86	Mo 80-93	Tc 47-50	Ru*(d^7s) 72-93	Rh*(d^8s) (95)-	Pd*(d^{10}) <145-	Ag 161-185	Cd 85-91
Ba 35-39	La 38-40, 50-52	Hf 51-79, 85-95	Ta 49-99	W*(d^4s^2) 49-99	Re 54-68	Os 67-(90)	Ir 75-109	Pt*(d^9s) 86-160	Au 121-160	Hg 108-126
Ra 37-48	Ac 39-68									

Table 5. Promotion Energies of $d^{n-1}s$ Valence State (in kcal per mole)

Ground-state configurations									
s^2	ds^2	d^2s^2	d^3s^2 except*	d^5s except*	d^5s^2	d^6s^2 except*	d^7s^2 except*	d^8s^2 except*	$d^{10}s$
Mg 137									
Ca 58	Sc 33,51	Ti 19,40	V 6-7	Cr 0	Mn 49-50	Fe 20-23,50-51	Co 10-15,43-46	Ni 1-5	Cu 0
Sr 52	Y 31-33,44	Zr 14-17,31-32	Nb* (d^4s) 0-3	Mo 0	Tc 7-12	Ru* (d^7s) 0-9,25-27	Rh* (d^8s) 0-10,26-31	Pd* (d^{10}) 10-29	Ag 0
Ba 26-27	La 8-12,21-22	Hf 40-51,59-64	Ta 28-38	W* (d^4s^2) 8	Re 34-49	Os 15-37,44-(51)	Ir 8-34,37-48	Pt* (d^9s) 0-29	Au 0
Ra 37-42	Ac (15-20),26-35								

BIBLIOGRAPHY

1. Born, Handbuch der Physik, XXXIV, 12.

2. Madelung, E., Zeits für Physik 11 (1910), 89, 8.

3. Goldschmidt, V. M., Z. Phys. Chem. Abt A 133 (1928), 397.
Goldschmidt, V. M., Kristallchemie und Röntgenforschung, Ergebnisse der Technischen Röntgenkunde, Leipzig, Akad, Verlagsgesselschaft, 1931.
Goldschmidt, V. M., Kristallchemie, Handbuch Naturwiss, 15 (1934).

4. Lewis, G. N., Journ. Am. Chem. Soc. 38 (1916) 762., Journ. Chem. Phys. 1 (1933) 17.

5. Lewis, G. N., Die Valenz und der Bau der Atome und Molekule, Vieweg & Sohn, Braunschweig, 1927.

6. Linnett, J. W., Am. Scientist 52 (1964), 459.

7. Hume-Rothery, W., Atomic Theory for Students of Metallurgy, Inst. of Metals, London, 1948.
Hume-Rothery, W., The Structure of Metals and Alloys, Inst. of Metals, London, 1936.

8. Drude, P., Ann Physik 1 (1900) 566; 3(1900) 370; 7 (1902) 687.

9. Lorentz, H. A., Proc. Acad. Amsterdam 7 (1905) 438, 585, 684.

10. Sommerfeld, A., Zs. Physik 47 (1928) 1.
Sommerfeld, A. and Bethe, H., Elektronentheorie der Metalle, Handbuch der Physik, Vol 24/2 (1933), 333.

11. Bloch, F., Zeits für Physik 52 (1928) 555; 59 (1930) 208.

12. Brillouin, L., Die Quantenstatistik und Ihre Anwendung auf die Elektronentheorie der Metalle, Springer, 1931.

13. Seitz, F., The Modern Theory of Solids, McGraw-Hill Book Co., Inc., New York, 1940.

14. Pauling, L., The Nature of the Chemical Bond, Third Edition, Cornell University Press, Ithaca, 1960.

15. Mott, N. F. and Jones H., The Theory of Properties of Metals and Alloys, Clarendon Press, Oxford, 1936.

16. Engel, N. N., "Survey over Bonding Theories," in "Phase Equilibria in Metallic Systems."

17. Heisenberg, W., Zeitschnift für Physik 33 (1925), 879.

18. Schrödinger, E., Annalen der Physik 79 (1926) 361, 489, 734; 80, 437; 81, 109.

19. Engel, N. N., Kemisk Maanedsblad 30 (1949), 53, 97.
Engel, N. N., Das Kubisch Raumzentrierte Gitter als Einelektronphase, "Radex-Rundschau" Heft 3, 1956.

20. Brewer, L., Prediction of High Temperature Metallic Phase Diagrams, UCRL-10701, University of California, July 1963.
Brewer, L., "Thermodynamic Stability and Bond Character in Relation to Electronic Structure and Crystal Structure" in Electronic Structure and Alloy Chemistry of the Transition Elements, Interscience, New York, 1963.

21. Engel, N. N., "Energy Wave Hypothesis."

22. Engel, N. N., Die Bindung erklärt durch Felder und Krafte, "Radex-Rundschau," Heft 1, 1956.

23. Engel, N. N., "Metallic Lattices Considered as Electron Concentration Phases," ASM Transactions Quarterly, Vol 57, No. 3, Sept. 1964.
Engel, N. N., "Copper, Copper Alloys and the Electron Concentration Concept," ACTA Metallurgica, Vol. 15, March 1966.

24. Hund, Eng. d exact Naturwissenschaften 8 (1929),147.

25. Heitler, W. and London, F., Zs. für Physik 44 (1927),455.

26. Hartree, D. R., Proc. Cambridge Phil. Magz. 24 (1928),89.

27. Engel, N. N., "Energy Wave Hypothesis," (to be published soon); by permission of author.

28. Rocca, Roberto and Bever, M. B., "The Thermoelastic effect in Iron and Nickel as a function of temperature," Trans. A. I.M.E., Vol. 188, Feb., 1950.

29. Thomson, W. (Lord Kelvin), Trans. Roy. Soc. Edin. (1853), 20, 261; Coll. Works, Cambridge (1882), 1, 174.

Thomson, W. (Lord Kelvin), Quart. Jl. of Math. (1857), 1, 55; Coll. Works, Cambridge (1882), 1, 291.

30. Liu, J., "Electron Movements in Metals Under Stress," M.S. (Met.) Thesis, Georgia Tech, March, 1970.

31. "Diffusion in Body-Centered Cubic Metals," International Conference on Diffusion in Body-Centered Cubic Materials, Gatlinburg, Tennessee, September 1964, A.S.M.